BRNO UNIVERSITY OF TECHNOLOGY

FACULTY OF MECHANICAL ENGINEERING

INSTITUTE OF MATERIALS SCIENCE AND ENGINEERING

PREPARATION OF THIN WALL CERAMIC HOLLOW FIBERS BY DIP-COATING

PŘÍPRAVA TENKOSTĚNNÝCH DUTÝCH KERAMICKÝCH VLÁKEN METODOU POVLAKOVÁNÍ NAMÁČENÍM

MASTER'S THESIS
DIPLOMOVÁ PRÁCE

AUTHOR   Bc. Radek Gockert
AUTOR PRÁCE

SUPERVISOR   doc. Ing. David Salamon, Ph.D.
VEDOUCÍ PRÁCE

BRNO 2017

Zadání diplomové práce

Ústav:	Ústav materiálových věd a inženýrství
Student:	**Bc. Radek Gockert**
Studijní program:	Aplikované vědy v inženýrství
Studijní obor:	Materiálové inženýrství
Vedoucí práce:	**doc. Ing. David Salamon, Ph.D.**
Akademický rok:	2016/17

Ředitel ústavu Vám v souladu se zákonem č.111/1998 o vysokých školách a se Studijním a zkušebním řádem VUT v Brně určuje následující téma diplomové práce:

Příprava tenkostěnných dutých keramických vláken metodou povlakování namáčením

Stručná charakteristika problematiky úkolu:

Příprava tenkostěnných dutých keramických vláken metodou povlakování namáčením je nový a technologicky náročný proces vyžadující volbu vhodné šablony a zároveň zvládnutí kontroly parametrů povlakování. Základními zvolenými materiály s vysokým aplikačním potenciálem jsou hydroxyapatit a oxid titaničitý. Připravená tenkostěnná dutá keramická vlákna pak mohou sloužit jako mikro kanálky pro přenos médií v živé tkáni (hydroxyapatit), nebo jako vhodný způsob imobilizace foto-katalytického materiálu (oxid titaničitý).

Cíle diplomové práce:

Experimentálně ověřit možnosti metody povlakování namáčením pro přípravu tenkostěnných dutých keramických vláken. Charakterizovat mikrostrukturu a tvar připravených vláken, zejména v závislosti na zvoleném slinovacím režimu a způsobu namáčení.

Seznam doporučené literatury:

Salamon, D., Chlup, Z., Lefferts, L. and Wessling, M. Tailoring of free standing microchannels structures via microtemplating, Mater. Res. Bull., 2011, 46, 505-511.

Lu, X., Lee, Y., Yang, S., Hao, Y., Evans, J. R. G. and Parini, C. G. (2010) Solvent-based paste extrusion solid freeforming, J. Eur. Ceram. Soc. 30, 1-10.

Salamon, D., Teixeira, S., Dutczak, S. M. and Stamatialis, D. F. Facile method of building hydroxyapatite 3D scaffolds assembled from porous hollow fibers enabling nutrient delivery, Ceram. Int., 2014, 40, 14793-14799.

Termín odevzdání diplomové práce je stanoven časovým plánem akademického roku 2016/17

V Brně, dne

L. S.

--   --

prof. Ing. Ivo Dlouhý, CSc.   doc. Ing. Jaroslav Katolický, Ph.D.

ředitel ústavu   děkan fakulty

ABSTRACT

This master thesis deals with the production of ultrathin ceramic hollow fibers by dip-coating. Preparation of ceramic hollow fibres is nowadays limited by dimension of outer and inner diameter. Application of dip-coating for preparation of ultrathin hollow fibers is new and technologically demanding process that requires the choice of a suitable sacrificial template, while mastering the control of coating parameters. The basic materials selected with high application potential are hydroxyapatite and titanium dioxide. Self-supporting hollow fibers with wall thickness below 1 µm were successfully prepared from both materials. Furthermore, dip-coating process of thin sacrificial templates was described. This method is unique because it allows the production of ultrathin ceramics fibers with an outside diameter below 100 µm and a wall thickness below 1 µm.

KEY WORDS
dip-coating, ultrathin ceramic hollow fibers, hydroxyapatite, titania

ABSTRAKT

Tato diplomová práce se zabývá výrobou ultratenkých keramických dutých vláken pomocí metody povlakování namáčením. Příprava keramických dutých vláken je v současnosti limitována rozměrem vnějšího a vnitřního průměru. Aplikace metody povlakování namáčením pro přípravu ultratenkých dutých je nový a technologicky náročný proces vyžadující volbu vhodné šablony a zároveň zvládnutí kontroly parametrů povlakování. Základními zvolenými materiály s vysokým aplikačním potenciálem jsou hydroxyapatit a oxid titaničitý. Samonosná dutá vlákna s tloušťkou stěny pod 1 µm byla úspěšně připravena z obou materiálů. Dále byl také popsán proces povlakování namáčením obětovaných šablon. Tato metoda je unikátní, protože umožňuje produkci ultratenkých keramických dutých vláken s vnitřním průměrem pod 100 µm a tloušťkou stěny pod 1 µm.

KLÍČOVÁ SLOVA
povlakování namáčením, ultratenká keramická vlákna, hydroxyapatite, oxid titaničitý

BIBLIOGRAPHIC CITATION

DECLARATION

I declare that this master´s thesis was worked out on my own using mentioned literature and under the supervision of above named supervisor.

In Brno on the 26th of May 2017 ....

Radek Gockert

ACKNOWLEDGMENT

CONTENTS

1 INTRODUCTION

The term *ceramic* comes from the Greek word *keramikos,* which means "burnt stuff," indicating that desirable properties of these materials are normally achieved through a high-temperature heat treatment process called firing. Up until the past 60 or so years, the most important materials in this class were termed the "*traditional ceramics,*" those for which the primary raw material is clay, products considered to be traditional ceramics are china porcelain, bricks, tiles, and, in addition, glasses and high-temperature ceramics [1].

The interest in recent years has focused on "*advanced ceramics,*" ceramics that with minor exceptions have been developer within the last decades. Advanced ceramics include ceramics for electrical, magnetic, electronic, and optical applications (sometimes referred to as "*functional ceramics*") and ceramics for structural applications at ambient as well as at elevated temperatures "*structural ceramics*" [2].

Ceramics materials are inorganic nonmetallic materials containing metallic and nonmetallic elements bonded by ionic and ionic-covalent bonds. Characteristic properties of ceramics with ionic-covalent bonds are high hardness, excellent chemical resistance, negligible ductility, low thermal conductivity and not significant electrical conductivity. Ionic ceramics tend to form closed packed structure similar to metals, but they have no free electrons, resulting in low electrical conductivity [3].

Ceramics have many applications, at a given application one property may be of the particular importance, but in fact, all relevant properties need to be considered. General interest is in combinations of properties [2].

Ceramics used for the repair and reconstruction of diseased or damaged parts of human body are termed bioceramics. With the growing demands of bioactive materials for orthopaedic as well as maxillofacial surgery, the utilization of calcium hydroxyapatite as fillers, spacers, and bone graft substitutes has received great attention mainly during the past two decades, primarily because of their biocompatibility, bioactivity, and osteoconduction characteristics with respect to host tissue. Dip-coating method appears to be one of the options shaping hydroxyapatite [4; 5].

TiO_2 powders have been commonly used as white pigments from ancient times. Their other outstanding feature is the photocatalytic effect. Photo catalysis has recently become a common word and various products using photocatalytic functions have been commercialized. Among many candidates for photo catalysts, TiO_2 is almost the only material suitable for industrial use at present and also probably in the future. This is because TiO_2 has the most efficient photo activity, the highest stability and the lowest cost [6].

2. GOALS OF WORK

a) Description of selected forming methods, which is connected with preparation of thin wall ceramic hollow fibers by dip-coating.

b) Describe a method of dip-coating in the preparation of ceramic materials with a view to preparing the fibrous structures.

c) Experimentally prepare thin wall ceramic hollow fibers from hydroxyapatite and titania by dip-coating.

d) Describe the change in the microstructure of the prepared materials, depending on the conditions of the coating process and sintering.

3 THEORETICAL PART (LITERATURE REVIEW)

3.1 Selected forming methods

3.1.1 Tape casting

Tape casting is important ceramic fabrication technique, as the name implies, thin sheets of a flexible tape are produced by means of a casting process. These sheets are prepared from slips, this type of slip consists of a suspension of ceramic particles in an organic liquid that also contains binders and plasticizers that are incorporated to impart strength and flexibility to the cast tape. The actual tape is formed by pouring the slip onto a flat surface (of stainless steel, glass, a polymeric film, or paper); a doctor blade spreads the slip into a thin tape of uniform thickness, as shown schematically in Figure 1. Tape thicknesses normally range between 0.1 and 2 mm. The green tape is then subjected to sintering. Many commercially important electronic packages based on alumina substrates and millions of barium titanate capacitors are made using this type of tape casting process [1; 7].
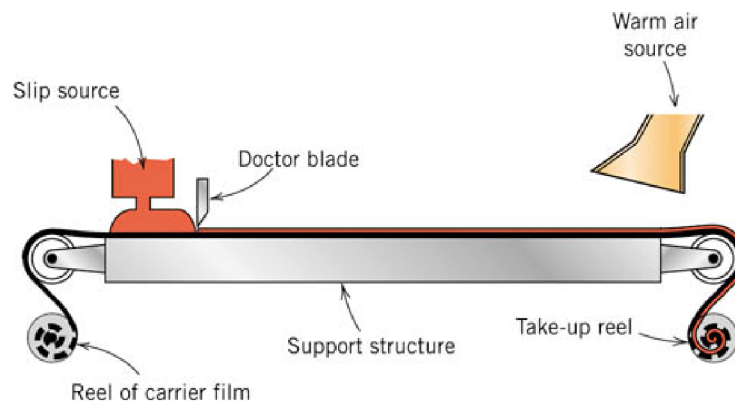

Figure 1. The scheme of tape casting method [1].

To achieve a high quality coating of ceramic on the substrate, the slurry must have the proper rheological characteristics, namely, pseudoplastic or shear-thinning behavior. This means that the viscosity is low when a high shear rate is applied, but the viscosity becomes high when the shear rate is low. The most common flaws that occur in the fabrication of these materials are longitudinal cracks, these may result from drying stresses or from pyrolysis process (to remove templates or sacrificial additives). Also thermal expansion differences between template and ceramic coating may lead to cracks at relatively low temperatures [8].

3.1.2 Sacrificial templates

Another way to produce porous ceramics is by mixing of appropriate amount of ceramics powder and material, which is in the subsequent process sacrificed. The biphasic composite containing a continuous ceramic matrix and a homogenously dispersed sacrificial phase, the composite is usually prepared by pressing a power mixture of the two components, slip, tape or direct casting of two-phase suspension, or impregnation of previously consolidates preforms of the sacrificial material with a preceramic polymer or ceramic suspension. Pore forming agents can be synthetic organic matters (polymer beads), natural organic matters (starch, sucrose, gelatine, and cellulose), inorganic matters (nickel, carbon, glass particles, etc.) and liquid (water) [9; 10].

Organic fugitives are usually extracted by pyrolysis (200-600 °C). During this process, the huge amount of generated gas can lead to a crack formation, thus burning rate must be slow enough. Ceramic and metallic particles are usually extracted by chemical way (e.g. acidic leaching) [9; 10].

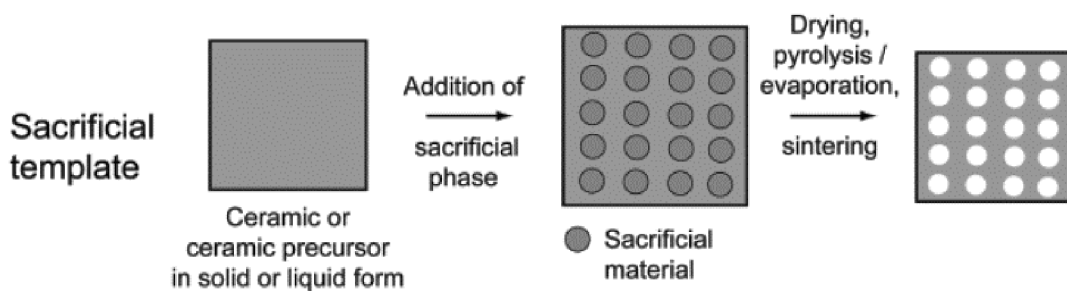The whole process of sacrificial fugitives is illustrated in Figure 2.

Figure 2. Principle of sacrificial fugitives [9].

Porosity is controlled by the amount of the agents, and pore shape and size are also affected by the shape and size of the agents respectively when their sizes are large in comparison with those of starting powders or matrix grains. This approach is useful particularly for obtaining of high open porosity. The agents, however, need to be mixed with ceramic raw powder homogeneously for obtaining uniform and regular distribution of pores [11].

In the present work, by using of sacrificial fibers, we can achieve infinitely long pore -shape microchannel. A channel structure can be created in the bulk ceramic material or ceramic hollow fibers can be self-supporting. The applied procedure is basically the sacrificial template process.

3.1.3 Free standing ultrathin ceramics

Ceramic thin films are used in various applications for their structural or functional properties. Below a thickness order of micrometers, ceramic films are typically deposited, sintered, and used on a supporting substrate due to their fragility. Literature reports versatile green film deposition and sintering techniques that allow the fabrication of free-standing structures [12]. This concepts are not limited to the materials used here and can potentially be extended to most ceramic materials and glasses. So prepared free-standing ultrathin ceramic foils allow new assembly and fabrication methods of devices and novel materials that contain thin ceramic membranes.

The fabrication of these foils basically consists of three main challenges: the substrate, the green film deposition method, and the sintering set up and conditions. The requirements for each of these processing steps, the most promising solutions, and the possible alternatives are illustrated in Figure 3 [12]. In the present work, sintering set up and conditions are simplified and the main focus in on film deposition method and a template selection.
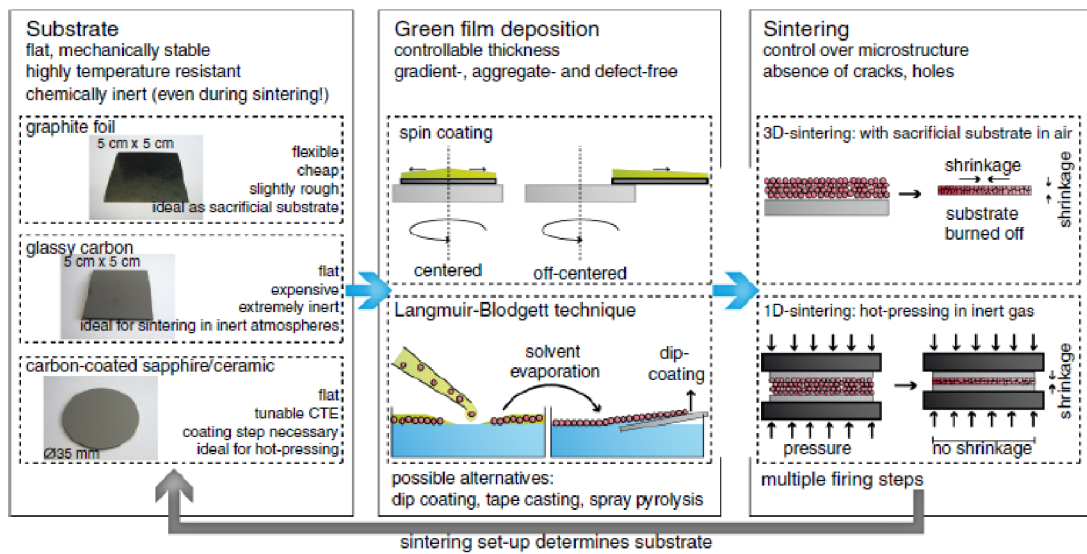

Figure 3. Fabrication of the free-standing ultrathin ceramic foils including the requirements and the solutions used for each processing step [12].

3.2 Suspensions and their physical properties

One of the ways to create ceramic green body is wet way. For this purpose it is necessary to produce slurry containing ceramic powder. Then we need stabilize suspension and add other substances that play an important role in the production of green body. Issues of preparation of suspensions and their physical properties will be discussed in the following chapters.

3.2.1 Solvents

The selection of a solvent involves basically a choice between water and an organic liquid. Organic solvents generally have higher vapor pressure, lower latent heat of vaporization, lower boiling point, and lower surface tension than water, due in a large part to the strong hydrogen bonding of the water molecules. The actual choice of a liquid for a given application often involves the consideration of a combination of several properties: the ability to dissolve other additives, evaporation rate, ability to wet the powder, viscosity, reactivity towards the powder, safety, and cost [2].

Evaporation rate is an important factor in the industrial tape casting where the tape is often cast, dried, peeled off from the carrier film, and rolled up for storage in a continuous operation. Fast drying solvents such as toluene and methyl ethyl ketone are commonly used for tape casting, particularly for thick tapes. Water is used occasionally for thin tapes, but has a distinct advantage over organic solvents when safety, cost, and waste disposal are considered [2].

3.2.2 Stabilization of suspension and zeta potential

The fundamental problem of suspension production is its stabilization. Two basic problems stabilizing suspensions are weight of ceramic particles and attractive Van der Walls forces between them. Firstly, the heavy particles are effected by gravitational forces, which lead to the sedimentation of the ceramic powder. The second important factor is presence of Van der Walls forces between particles. If are these forces large, particles create large colagulates, which tend sedimented [2].

Colloidal stability is governed by the total interparticle potential energy, V_{total}, which can be expressed as:

$$V_{total} = V_{vfW} + V_{elect} + V_{steric} + V_{structural}, \tag{3.1}$$

where V_{vdW} is the attractive potential energy due to long-range van der Waals interactions between particles, V_{elect} the repulsive potential energy resulting from electrostatic interactions between like-charged particle surfaces, V_{steric} the repulsive potential energy resulting from steric interactions between particle surfaces coated with adsorbed polymeric species, and $V_{structural}$ the potential energy resulting from the presence of non-adsorbed species in solution that may either increase or decrease suspension stability. The first two terms of equation (3.1) constitute the well-known

DLVO theory developed by Derjaguin, Landau, Verwey and Overbeek. This theory, which predicts the stability of colloidal particles suspended in polar liquids, is a cornerstone of modern colloid science [13].

There are several ways for achieving stabilization of suspension, but the most commonly used are [2]:

1. *Electrostatic stabilization* in which the repulsion between the particles is based on electrostatic charges on the particles

2. *Steric stabilization* in which the repulsion is produced by uncharged polymer chains adsorbed onto to the particle surfaces

3. *Electrosteric stabilization*, consisting of a combination of electrostatic and steric repulsion, achieved by the adsorption of charged polymers (polyelectrolytes) onto the particle surfaces.
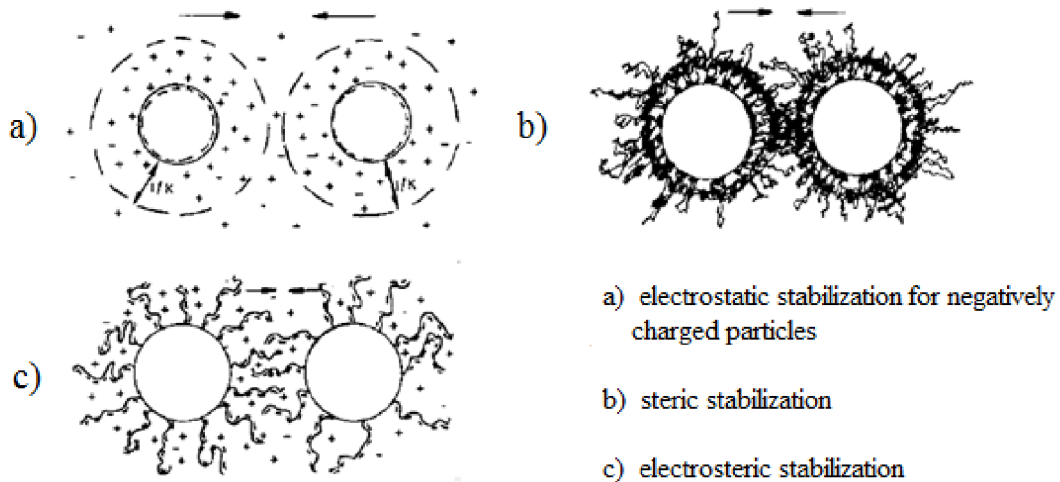

a) electrostatic stabilization for negatively charged particles

b) steric stabilization

c) electrosteric stabilization

Figure 4. Schematic ilustration commonly used stabilizations [2].

Electrostatic stabilization, as outlined above, is said to occur when the repulsion between the particles is achieved by electrostatic charges on the particles (Figure 4a). The repulsion is not, however, a simple case of repulsion between charged particles. An electrical double layer of charge is produced around each particle, and the repulsion occurs as a result of the interaction of the double layers. *Steric stabilization* is the term used to describe the stabilization of colloidal particles which results from the interaction between uncharged polymer chains adsorbed onto the particle surfaces (Figure 4b). The interactions between the polymer chains are fundamentally different from those between the charged ions in electrostatic stabilization and are dominated by the configurational entropy of the chains. As outlined earlier, suspensions can also be stabilized by *electrosteric repulsion*,

involving a combination of electrostatic repulsion and steric repulsion (Figure 4c). Electrosteric stabilization requires the presence of adsorbed polymers and significant double layer repulsion. It is commonly associated with suspensions in aqueous liquids. A common way of achieving electrosteric stabilization in aqueous liquids is through the use of polyelectrolytes,i.e., polymers that have at least one type of ionizable group (e.g., carboxylic or sulfonic acid group) that dissociates to produce charged polymers [2].

During stabilizing the suspension containing nanopowders it is necessary to take into account the shape and size of the particles and therefore it is necessary to take into account the raw powder production technology [14].

One of the ways to characterize this stabilization is the zeta potential (ζ) which expresses the tension at the interface between particles and solvent. This interphase parameter is influenced by the properties of the particle surface and the solvent. Zeta potential is usually expressed in milivolts and illustrates the voltage between electrical double layers of particles in the suspension and prevents their approach. Zeta potential can be measured by the Electrokinetic Sonic Amplitude (ESA) method [15].

Another important factor in the preparation of suspensions is pH. Each colloidal suspension has a different value of the zeta potential for different pH, change pH can tend to higher zeta potential and better stabilization of suspension. Another factor is the conformation of stabilizing polymer, which varies with the changing pH as shown in Figure 5. DLVO theory predicted dispersions can be rendered unstable by adjusting pH toward the isoelectric point (IEP). Values for selected materials are in Table 1 [13; 16].
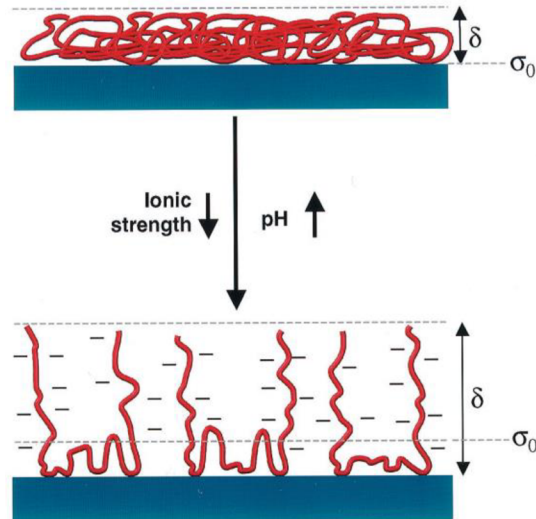
Figure 5. Schematic illustration of adsorbed anionic polyelectrolyte species on an ideal ceramic surface as a function of pH and ionic strength (δ is the added layer thickness and σ_o the plane of charge) [13].

Table 1. Isoelectric points of ceramic materials [13].

Material	IEP
α-Al_2O_3	8-9
$3Al_2O_3 \times 2SiO_2$	6-8
$BaTiO_3$	5-6
CeO_2	6.7
Cr_2O_3	7
CuO	9.5
Fe_3O_4	6.5
La_2O_3	10.4
MgO	12.4
MnO_2	4-4.5
NiO	10-11
SiO_2 (amorphous)	2-3
Si_3N_4	9
SnO_2	7.3
TiO_2	4-6
ZnO	9
ZrO_2	4-6

In the Figure 6 we can see impact dispersant and pH on hydroxyapatite suspension, it is clear that suspension is stabilized in the range 11-12 pH, where the absolute value of the zeta potential is the highest. It is also seen that use of the dispersant Does not have such an effect in this range of pH. Another factor may be the size and shape of the particles, this influence can be seen in Figure 7. In this case, the use of suspensions without stabilization and stabilized through sodium dodecyl benzene sulfonate (DBS) and hydroxypropyl methyl cellulose (HPMC).
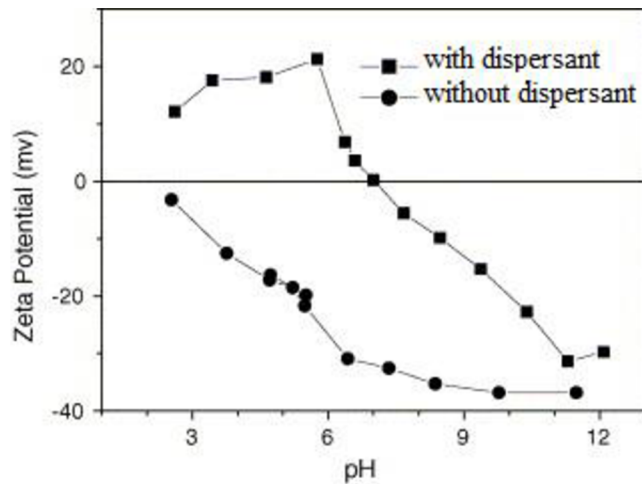

Figure 6. The effect of pH and dispersant on the zeta potential of hydroxyapatite suspensions [16].
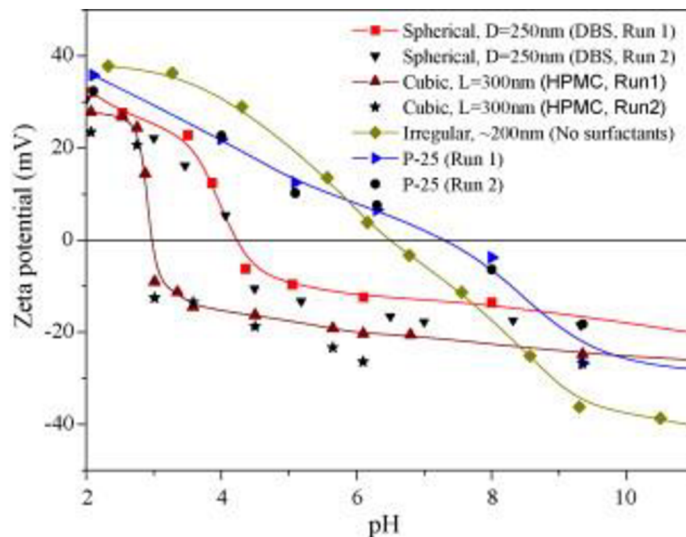

Figure 7. The influence of size, shape and dispersant on the zeta potential of titania suspension [14].

3.2.3 Binders and plasticizers

Binders are typically long chain polymers that serve the primary function of providing strength to the green body by forming bridges between the particles. In some forming methods (e.g., injection moulding), they also provide plasticity to the feed material to aid the forming process. The selection of a binder for a given forming process involves the consideration of several factors that include binder burnout characteristics, molecular weight, glass transition temperature, compatibility with the dispersant, effect on the viscosity of the solvent, solubility in the solvent, and cost [2].

Plasticizers are generally organic substances with a lower molecular weight than the binder. The primary function of the plasticizer is to soften the binder in the dry state, thereby increasing the flexibility of the green body (e.g., tapes formed by tape casting). For forming processes in which the binder is introduced as a solution, the plasticizer must be soluble in the same liquid used to dissolve the binder. In the dry state, the binder and plasticizer are homogeneously mixed as a single substance. The plasticizer molecules get between the polymer chains of the binder, thereby disrupting the chain alignment and reducing the van der Waals bonding between adjacent chains. This leads to softening of the binder but also reduces the strength [2].

3.2.4 Viscosity

The viscosity of a fluid (η) is a measure of how resistive the fluid is to flow. For example, thick honey is more resistive to flow than water, and so honey is more viscous than water. Viscosity is the fluid analogy of friction between solids; both are mechanisms by which the kinetic energy of moving objects can be transferred to thermal energy. In the absence of friction, a block could glide at constant speed along a horizontal surface. In the same way, an object moving through a nonviscous fluid would experience no viscous drag force, that is, no resistive force due to viscosity; it could move at constant speed through the fluid [17].

For an ideal fluid is assumed absence of shear-shear stress. For real liquid this is only applies if the fluid is not moving. If the fluid flows and the individual elementary volumes (molecules) are in relative motion and two adjacent layers have a different speed. The interface between the two layers to form friction and to produce shear stress, causing this phenomenon is the viscosity of the fluid. For laminar flow Newton formulated the law under which the tangential stress in the fluid proportional to the dynamic viscosity and velocity gradient. Newton's law of viscosity is formulated by equation 3.2 [18].

$$\tau = \eta \frac{du}{dx},\qquad\qquad\qquad(3.2)$$

where: τ is shear stress,   [Pa]

η is dynamic viscosity, [Pa s]

du/dx is velocity gradient. [s^{-1}]

The above equation is valid for the liquid which is called Newtonian. Adding ceramic powder, however, the suspension becomes non-Newtonian [2], this means that viscosity depends on the velocity gradient, and viscosity should be measured for different values of velocity gradients. This is illustrated in Figure 8.
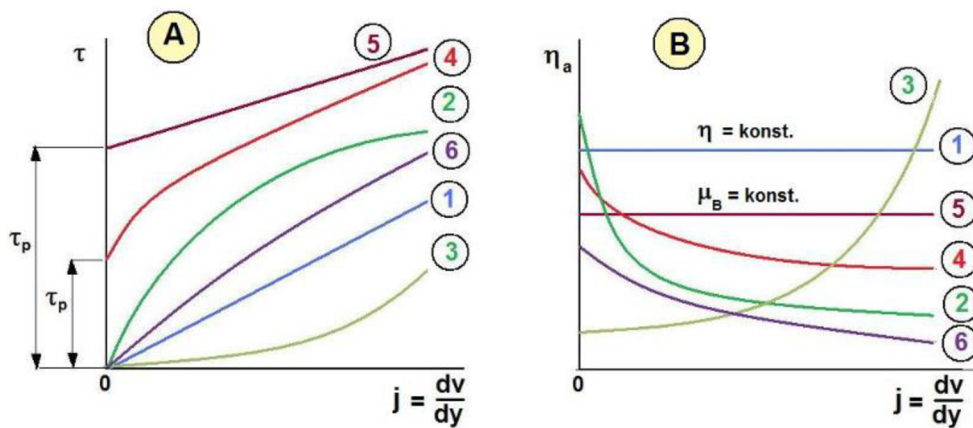

Figure 8. Rheograms (A) and dynamic viscosity (B) depending on the velocity gradient [18].

1 - Newtonian fluid, 2-6 - non-Newtonian fluid

2 - pseudo-fluid, 3 - dilatant fluid, 4 - real plastic fluid, 5 - Binghams ideally plastic fluid, 6 - Eyrings model of fluid

Characteristics of non-Newtonian liquids are shown in Table 2.

Table 2. Characteristics of non-Newtonian liquids [18].

Non-Newtonian fluid	Description	Example
Pseudo-fluid	Drop in apparent viscosity with an increasing shear stress	Asymmetrical suspension of particles, colloidal solution, the solution, polymer, rubber, ketchup, whipped cream
Dilatant fluid	Increase of apparent viscosity with increasing shear stress	Paints, solvents of paints, starch pastes, concrete, gum Arabic, honey
Real plastic fluid	At rest, the fluid-dimensional structure having a rigidity capable of resisting any stress less than the stress on the deformation. After this the stress across the fluid behaves as a Pseudo-fluid.	Some clays, some mugs, mayonnaise
Binghams ideally plastic fluid	At rest, the fluid-dimensional structure having a rigidity capable of resisting any stress less than the stress on the deformation. After this the stress across the fluid behaves as a Newtonian.	Concentrated slurry, granular slurry, mud, pastes, paints oleaginous, blood, toothpaste
Eyrings model of fluid	These mode has two parameters and Eyring was derived from the kinetic theory of liquids, so it is a semi-empirical model, other models are only empirical	

For measuring the viscosity of Newtonian liquids, the following devices are used: capillary viscometers, viscometers outlet, ball viscometers, rotational viscometer, and vibration viscometers. Measuring the viscosity of non-Newtonian liquids is more difficult, viscosity is parameter of velocity gradient and it is necessary to measure different values of velocity gradient, resulting rheogram, which express varying viscosity depending on the speed gradient. To measure the viscosity of non-Newtonian liquids it is therefore necessary to use the device with a clearly defined geometry flow and we can determine the value of the velocity gradient *du/ dx* and the corresponding value of shear stress. Conventional instruments for measuring non-Newtonian liquids by capillary viscometers are rotational viscometers [18].

3.2.5 Surface tension

Surface tension γ is defined as a force which acts perpendicularly to the length of an imaginary sectional surface, divided by the length and located in a plane tangent to the surface of the liquid. Considering this, if the surface of the line segment of length *L*, the two surface portions which are adjacent to it, at each force *F* applied, then [19]:

$$\gamma = \frac{F}{L} \ ,$$
(3.3)

where: γ is surface tension, $[N \times m^{-1}]$

F is force, $[N]$

L is length. $[m]$
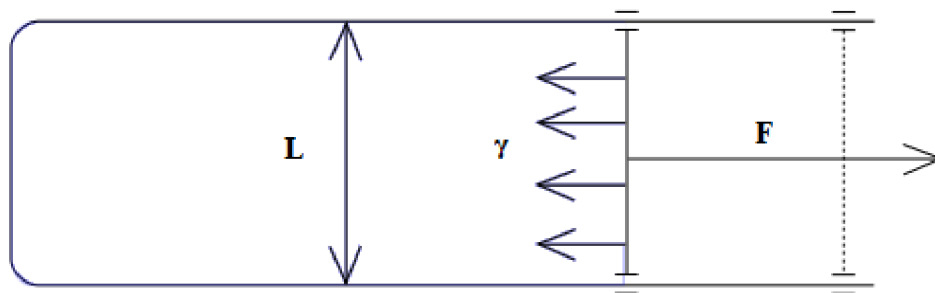
This equation is schematically illustrated in Figure 9.

Figure 9. Principle of surface tension [19].

Unit surface tension is therefore $[N \times m^{-1}]$, consequence is that to increase the surface work is needed. Surface tension, however, may also represent an areal density of the potential energy surface. In this case the surface tension is expressed in units $[J \times m^{-2}]$. [19]

In colloidal systems there are at least two different phases separated by phase boundary; properties of phase boundaries significantly affects the behavior of the whole system. Due to the interaction of molecules of solid particles in the colloid with molecules of liquid phase is clear that the surface molecules will have different characteristics from the volume molecules, it is apparent from Figure 10. Surface molecules are configured in such a shape that the surface energy is minimized. Changing the interface surface is associated with executing the work to be done in connection with a surface tension [20].
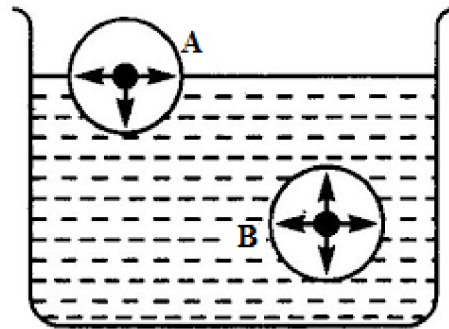

Figure 10. Different characteristics surface (A) and volume (B) molecules [19].

Surface energy or surface tension, can be easily measured at the mobile phase interface gas-liquid, respectively. liquid-solid. There are the following methods: *static, semi-static and dynamic*. When *static* methods is reached to equilibrium, resulting therefore the equilibrium value of the surface energy. This group includes the method capillary elevation method and sitting or hanging drop. The *semi-static* methods are working under conditions approaching equilibrium, so that the values of surface energy (surface tension) are very close to equilibrium. The most commonly used method are using maximum bubble pressure or stripping Pt-Ir ring. These methods allow the study of imbalances in multiphase systems that more correspond to real technological processes such as washing or lubrication of moving parts, painting operations and the like. The task of these methods, rather than measuring the surface energy or surface tension, is determination of wetting of the solid surface by liquid for dynamic conditions [20].

3.3 Material characteristics and applications

3.3.1 Hydroxyapatite (HAP) and biomedicine

Every year millions of people need a transplant of bone, therefore, the requirements for materials to replace them. These materials must have suitable mechanical properties, but also meet the requirements for biocompatibility. One material suitable for bone tissue engineering is hydroxyapatite [21]. Hydroxyapatite is the main inorganic component of bone and tooth of humans and animals, has been widely

investigated for applications in biomedical fields owing to its excellent biocompatibility. [22].

Hydroxyapatite is a non-resorbable calcium phosphate. Due to chemical composition and crystallography similarity to bone mineral, hydroxyapatite exhibits an excellent biocompatibility, and therefore this material is extensively studied for bone tissue application. Hydroxyapatite belongs to a group of bioactive ceramics, this means that it is osteoconductive and able to directly bond to bone. Hydroxyapatite is suitable in bone tissue engineering, however, its application is limited due to low mechanical strength and very slow biodegradation. Mechanical properties are influenced by porosity, crystallinity, grain size, and composition as well. The stiffness, strength and toughness can be enhanced by using crystalline, low porous small-grain-sized HAP [10].

Thermal stability of hydroxyapatite depends on number of factors such as the feedstock for the synthesis of the powder and its production technology. Decomposition of Hap to α-TCP (α tricalcium phosphate) and TTCP (tetracalcium phosphate) results in the changes in physicochemical properties of the final material. Hydroxyapatite thermal stability is mainly determined by two factors. First is the stoichiometry Ca/P ratio and structural substitutions and second is the gas composition during heating. At a temperature of 1050 °C occurs dehydroxylation and decomposition at 1250 °C. Thermal stability can be lowered the most by a substitution of calcium and phosphate, leading to loss in phase stability [23; 24].

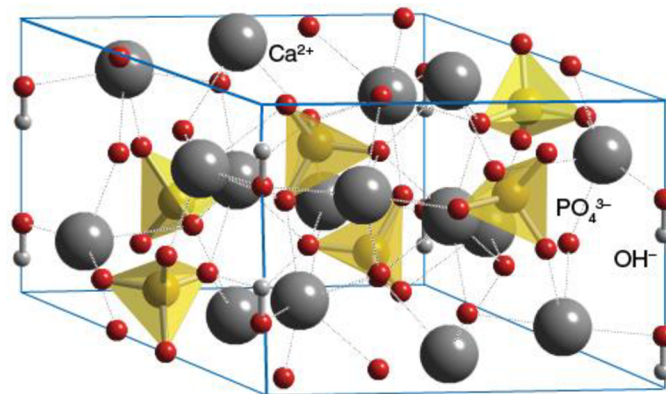Hydroxyapatite structure we can see in Figure 11.

Figure 11. Structure of hydroxyapatite [25].

3.3.2   Titania and photo catalysis

Since its commercial production in the early twentieth century, titania (TiO_2) has been widely used as a pigment and in sunscreens, paints, ointments, toothpaste, etc. In 1972, Fujishima and Honda discovered the phenomenon of photocatalytic splitting of water on a TiO_2 electrode under ultraviolet light (UV) 6-8. [26] Since then,

enormous efforts have been devoted to the research of TiO_2 material, which has led to many promising applications in area photo catalysis [26].

Word photo catalysis is composed of two words: photo = light and catalysis = process which is characterized in that a substance known as a catalyst facilitates the reaction rate. It must be said that photo catalysis takes place on the surface of semiconductors. From the different elemental semiconductors and other substances with semiconducting properties for photo catalysis best suited titania through suitable width forbidden gap. Irradiate semiconductor light quanta which have energy higher than the band gap energy occurs therein to form a pair of hole - electron. If a suitable acceptor does not capture these defects occur within a few nanoseconds to recombine. Life time of this process is not limited. This has the effect that the surface leads to decomposition of organic substances, these substances may be undesirable hydrocarbons or living organic substances such as bacteria, viruses or fungi. This property has use in areas with high demands on hygiene, such as hospitals [27].

Titania is a polymorphic material and exists in three structures: *rutile, anatase and brookite*. Rutile is the stable phase at high temperatures, but anatase and brookite are naturally common in fine grained (nanoscale). In a thermal process, and grain coarsening can be seen the structure of the following transformations: anatase to brookite to rutile, brookite to anatase to rutile, anatase to rutile, and brookite to rutile. These transformations are often dependent on particle size. For small TiO_2 nanoparticles (<50 nm), anatase is more stable and transformed to rutile at temperature >700 ℃ [26]. TiO_2 nanoparticles had anatase or brookite structures, which transformed to rutile after reaching a certain particle size. If rutile transformation to take place, rutil grew much faster than anatase. It was found that rutile became more stable than anatase for particle size > 14 nm [28].

There are two the unit cell structures, rutile and anatase. These two structures can be described in terms of chains of TiO_6 octahedra, where each Ti^{4+} ion is surrounded by an octahedron of six O^{2-} ions. These structures are shown on Figure 12. The properties of titania include, in particular its photo stability, corrosion resistance, non-toxicity, high photocatalytic activity and low price. For the purposes of the photocatalytic titania frequently in two forms - as a suspension of ceramic powder and in the form of a thin layer deposited on the substrate [26].
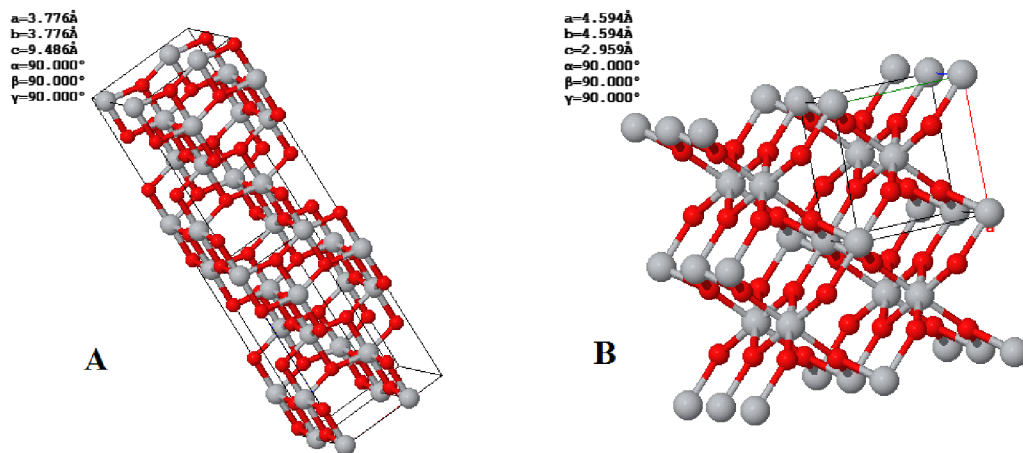
Figure 12. Lattice structure anatase (A) and rutile (B) [25].

3.4 Sintering

Sintering is a processing technique used to produce density-controlled materials and components from metal or ceramic powders by applying thermal energy. When thermal energy is applied to a powder compact, the compact is densified and the average grain size increases. The basic phenomena occurring during this process, called sintering, are densification and grain growth. This technique is one of the oldest human technologies, originating in the prehistoric era with the firing of pottery. These days, sintering is widely used to fabricate bulk ceramic components and powder metallurgical parts [29].

3.4.1 Driving force of sintering

Non-compacted ceramic body, which has not undergone heat treatment (sintering), is called a *green body*. This green body is formed by ceramic powder and compared to the solid body has a significantly greater surface area and surface energy $\Delta(\gamma A)$. This excess energy is the driving force for sintering, because the system tries to reduce this energy. It follows that what is the size of the ceramic powder is smaller, the specific surface area is larger and sintering proceeds rapidly. In order to reduce the surface energy process is started, it is necessary to supply the initial activation energy, that is generally supplied in the form of thermal energy. At high temperatures is made possible by the diffusion between ceramic particles and reducing the surface. During the sintering process, subsequently decreasing the volume and porosity of green body and leads to grain growth in the microstructure [3; 29]. Coarsening and densification of green body is shown in Figure 13.
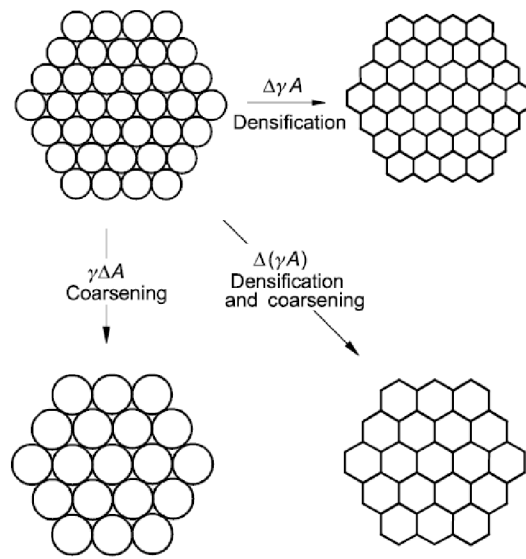
Figure 13. Basic phenomena occurring during sintering under the driving force Δ(γA) for sintering [29].

3.4.2 Diffusion

Many reactions and processes that are important in the treatment of materials rely on the transfer of mass either within a specific solid (ordinarily on a microscopic level) or from a liquid, a gas, or another solid phase. This is necessarily accomplished by diffusion, the phenomenon of material transport by atomic motion. From an atomic perspective, diffusion is just the stepwise migration of atoms from lattice site to lattice site. The atoms in solid materials are at high temperature in constant motion, rapidly changing positions. For an atom to make such a move, two conditions must be met: there must be an empty adjacent site, and the atom must have sufficient energy to break bonds with its neighbour atoms and then cause some lattice distortion during the displacement. At a specific temperature some small fraction of the total number of atoms is capable of diffusive motion, by virtue of the magnitudes of their vibrational energies. This fraction increases with rising temperature. Several different models for this atomic motion have been proposed; of these possibilities, two are dominant: *vacancy and interstitial* diffusion for metallic diffusion [1]. Both models are represented schematically in Figure 14.
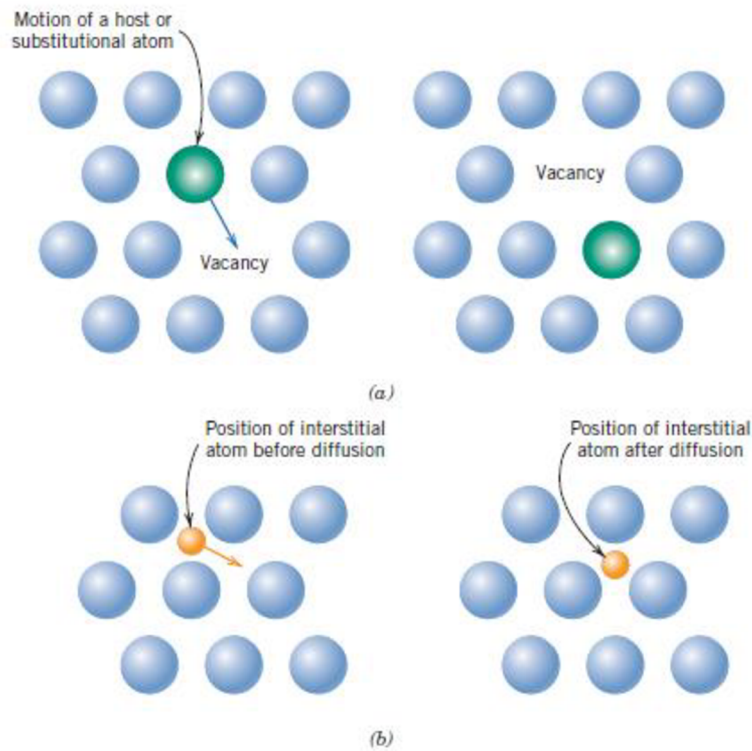
Figure 14. Schematic representations of (a) vacancy diffusion and (b) interstitial diffusion. [1]

In the case of ceramic materials and sintering it is necessary to take into account the grain boundary diffusion. This is shown in Figure 15 [30].
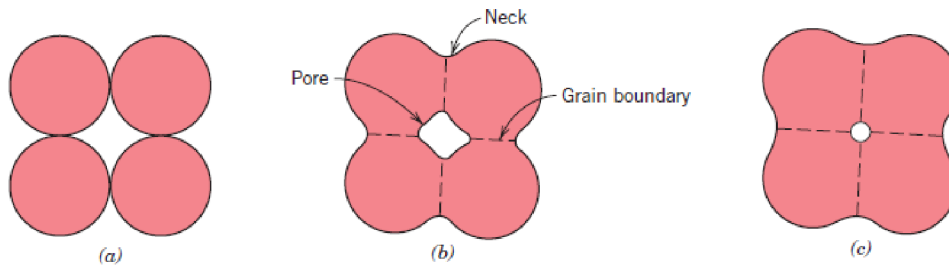

Figure 15. Schematic representations of grain boundary diffusion (a) particles after pressing, (b) particle coalescence and pore formation as sintering begins, (c) as sintering proceeds, the pores change size [1].

During diffusion decreases the concentration differences which movement usually takes place on locations with a higher concentration to locations with a lower concentration. The mathematical description of the diffusion process is described by Fick's laws. *First Fick law* gives the diffusion flux *J* as the amount of diffusing agents with diffusion coefficient *D* which, when the concentration gradient *dc/dx*

passes through a unit area (1 m^2) perpendicular to the direction of diffusion per unit time dτ = 1s. Mathematical expression of Fick's law is described in equation 3.4. Fick's first law, however, can only be used if the concentration gradient does not change in time [31].

$$J = -D\frac{dc}{dx},$$ (3.4)

where: J = diffusion flux,   [kg × m^{-2} × s^{-1}],

          D = coefficient,   [m^2 × s^{-1}],

          dc/dx = concentration gradient.   [kg × m^{-4}].

Second Fick law considering the volume concentration c [kg m^{-3}] diffusing substance and its change depending on time and location. The second Fick's law is derived using Fick's first law, and with regard to the law of conservation of mass. This law allows for changing the concentration gradient and the final mathematical solution, it is necessary to determine the boundary conditions. Second Fick's law for unidirectional diffusion in the x-axis direction in the exact shape, is also called as differential equations of diffusion and is illustrated by the equation 3.5 [31].

$$\frac{\partial c}{\partial \tau} = \frac{\partial}{\partial x}\left(D\frac{\partial c}{\partial x}\right),$$ (3.5)

where the variables are defined as variables in the first Fick's law.

3.4.3   Partial sintering

Partial sintering is the simplest method suitable for processing of structures with randomly arranged irregular pores. Pore size and porosity can be controlled by the pore size of a raw powder and by sintering conditions like lower temperature and shorter time than required for full densification. The resulting pores are too small to allow bone tissue penetrate inside thus this technique cannot be used separately in tissue engineering. However, it can be convenient to combine this method with another [10].

3.5 Ceramic Fibers

Ceramic fibers can be essential components of new high-temperature-resistant lightweight materials. Manufacture of ceramic fibers is often difficult proces and in most cases polymeric components or structures are key factors for fiber spinning. Organic polymers are used as additives to produced oxid ceramic fiber and inorganic polymers are the precursors for the production of non-oxide ceramic fibers [32].

In this work will be presented basic methods for producing ceramic fibers and selected types of these fibers.

3.5.1 Classification of different types of fibers

The term ''ceramic fibers'' includes all non-metallic inorganic fibers (oxide or non-oxide) with the exception of fibers manufactured via solidification of glass melts. Difference between ceramic fibers and glass fibers became more difficult during the last years, because ceramics produced via new precursor or sol-gel routes can also be of amorphous structure and the production process can also contain a melt processing step. This means that ceramic fibers can be either polycrystalline, partially crystalline or amorphous, but the expression ''glass fibers'' should only be applied to fibers that are produced via solidification of typical glass melts based on silicate systems. If these melts are produced by using minerals like basalt, the fibers should be called ''mineral fibers''. Classification of different fiber types is shown in Figure 16 [33].
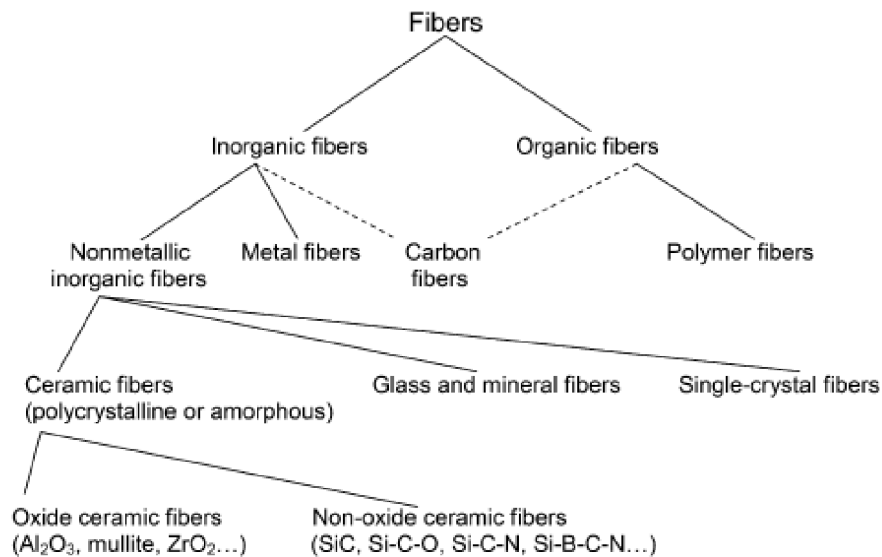

Figure 16. Classification of different fiber types [33].

3.5.2   Processing of fibers

Indirect fiber production

CVD process

Using this method are ceramic fibers formed by vapor deposition of ceramic material on the carrier fibers. This carrier fiber forms the core of the resulting ceramic fibers. Because the carrier material remains in the fiber, the resulting fibers are mostly thick, stiff, and difficult to process [32; 33].

Relic process

In relic proces absorbent organic fiber materials (mostly cellulose-based) are saturated with salt solutions or sols. Then will burn organic material and salt or salt is converted to ceramics [33].

Direct fiber production

Direct production processes can be identified by the preceramic precursor components used in the spinning dopes.

Spinning dopes based on molecularly dispersed precursors

In these processes soluble salts are used in the spinning dopes, which can be converted into ceramics during a calcination step. Salt is disolved in form of ions, which are disperzed. In addition to the salt, the spinning dope consists of organic polymers to achieve the rheological properties needed for the spinning process. Solvents are usually water or water/alcohol mixtures. In some cases it is possible to add nanoscaled ceramic particles to control the structure formation during ceramization. In this case, the process is called the "*solution process*" [32].

Spinning Dopes Based on Colloidally Dispersed Precursors

This process is similar to the one mentioned above, but here colloidal inorganic components are used as preceramic precursors. They are also used polymers to obtain rheological properties. The same solvenst are used as stated above. In this case, the process is called the "*sol/gel process*" [32].

Spinning Dopes Containing Coarse Ceramic Particles

Sometimes, coarse ceramic particles are added to salt or sol based spinning dopes in order to increase the ceramic yield and to reduce the shrinkage during calcinations and sintering. In this case, the process is called the "*slurry process*" [33].

In this case the spinning dope consists of either a solution of an inorganic polymer, which can be spun via a dry spinning process or the precursor polymers are meltable and can be spun using a melt spinning process. It is no need add polymer to adjustment of rheological properties. In this case, the process is called the "*precursor polymer process.*" The precursor polymer process technique is particularly applied for the production of non-oxide ceramic fibers [32].

Production route of ceramic fibers with facilities is shown in Figure 17.
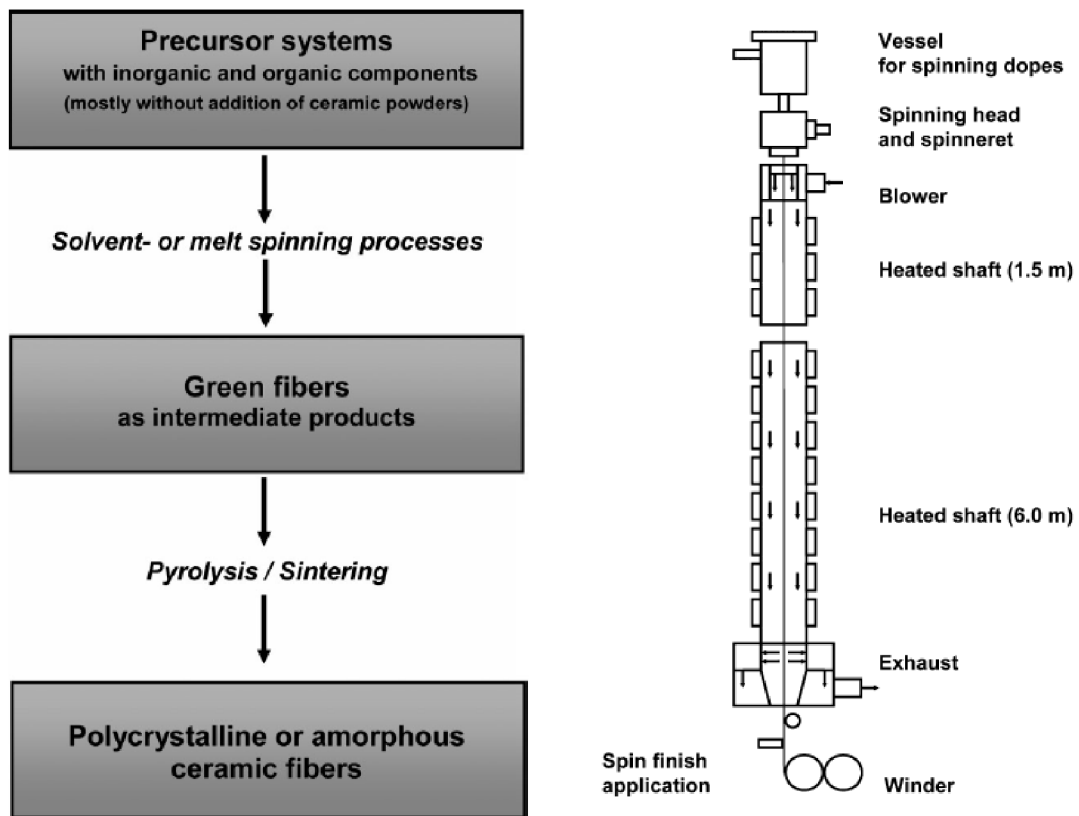
Figure 17. Production route of ceramic fibers with facilities [33].

3.5.3   Selected ceramic fibers

Oxide ceramic fibers

Known examples for oxide ceramic fibers are fibers made of aluminia (Al_2O_3), mullite (mixed oxides of Al_2O_3 and SiO_2), YAG (yttrium aluminum garnet, $Y_3Al_5O_{12}$), and zirconium dioxide (ZrO_2). All these fibers have a polycrystalline microstructure and are characterized by high values of tensile strength and modulus. Due to their oxidic nature they are stable against oxidation also at high temperatures. Although oxidation is not a problem for oxide fibers, creep, due to grain boundary sliding at high temperatures, is a limitation and is higher than for SiC-based fibers. Oxide

fibers which are currently available commercially are mostly based on Al_2O_3 or Al_2O_3/SiO_2 ceramics [32].

Overview of commercial oxide ceramics is shown in Table 3.

Table 3. Overview of commercial oxide ceramic fibers [33].

Trademark	Elemental composition	Diameter [μm]	Density [gcm^{-3}]	Production technique	Tensile strength [GPa]	Tensile modulus [GPa]
3M Nextel 720	Al_2O_3, SiO_2	10-12	3.4	sol/gel	2.1	260
3M Nextel 610	Al_2O_3	10-12	3.9	sol/gel	3.1	380
3M Nextel 550	Al_2O_3, SiO_2	10-12	3.03	sol/gel	2.0	193
3M Nextel 440	Al_2O_3, SiO_2, B_2O_3	10-12	3.05	sol/gel	2.0	190
3M Nextel 312	Al_2O_3, SiO_2, B_2O_3	10-12	2.7	sol/gel	1.7	150
Sumitomo Altex	Al_2O_3, SiO_2	10/15	3.3	polyalumi-noxane,	1.8	210
Nitivy Nitivy ALF	Al_2O_3, SiO_2	7	2.9	sol/gel	2.0	170
Mitsui Almax-B	Al_2O_3, SiO_2	7-10	2.9	unknown	not available	

Non-Oxide ceramic fibers

Non-oxide ceramic fibers are used for high temperature exhibit high values for tensile strength and modulus (higher than oxide fibers) and due to their structure, which is amorphous or polycrystalline, exhibit also lower creep rate at high temperatures than the polycrystalline oxide fibers. The use of non-oxide fibers is limited by their susceptibility to oxidative degradation. The lower the oxygen content of the fiber the better is the oxidation resistance. Commercially available non-oxide ceramic fibers are based on SiC and Si-C-O materials which contain undesirable oxygen to a greater or lesser extent and can also contain some percent of Ti, Zr, Al, or B [32].

Overview of commercial non-oxide ceramics is shown in Table 4.

Table 4. Overview of commercial non-oxide ceramic fibers [33].

Trademark	Manufacter	Approximate max. production temperature	Elemental composition	Average fiber diameter [μm]	Tensile strength [GPa]	Tensile modulus [GPa]
Nicalon NL 200/201	Nippon Carbon	1200	Si, C, O	14	3	220
Tyranno LoxM	Ube Industries	1200	Si, C, O, Ti	11	3.3	187
Tyranno S	Ube Industries	1200	Si, C, O, Ti	8.5/11	3.3	170
Hi-Nicalon	Nippon Carbon	1300	Si, C, O	14	2.8	270
Tyranno ZMI	Ube Industries	1300	Si, C, O	11	3.4	200
Hi-Nicalon S	Nippon Carbon	>1500	Si, C, O	12	2.6	420
Tyranno SA 1/3	Ube Industries	>1700	Si, C, O, Al	10/7.5	2.8	380
Sylramic	COI Ceramics	>1700	SiC, TiB_2, B_4C, O	10	2.7	310
Sylramic-iBN	COI Ceramics	>1700	SiC/BN	10	3.0	400

3.6 Dip-coating

Dip-coating is a simple method for coating any desired templates with a high potential for industrial use. The method can applied very thin films produced from the suspension in which is dispersed requested material. The films made by dip-coating have very good quality, the whole process is also economically very unpretentious [5].

3.6.1 Principle methods

Principle of the method is to form a suspension containing the desired material, such as ceramic powder. The suspension must be stabilized and substances homogeneously dispersed before the process start. The main characteristics of suspension for dip-coating are surface tension and viscosity. The coated template, in in this study is the thin fiber immersed in the suspension and subsequently is withdrawn out. During this process the template forms a coating whose thickness is determined by the properties of the slurry, template and setting of the dip-coating process. By selecting suitable parameters of the above aspects, we can achieve the required thickness of film. Principle of the method and real image of the process is shown in Figure 18.
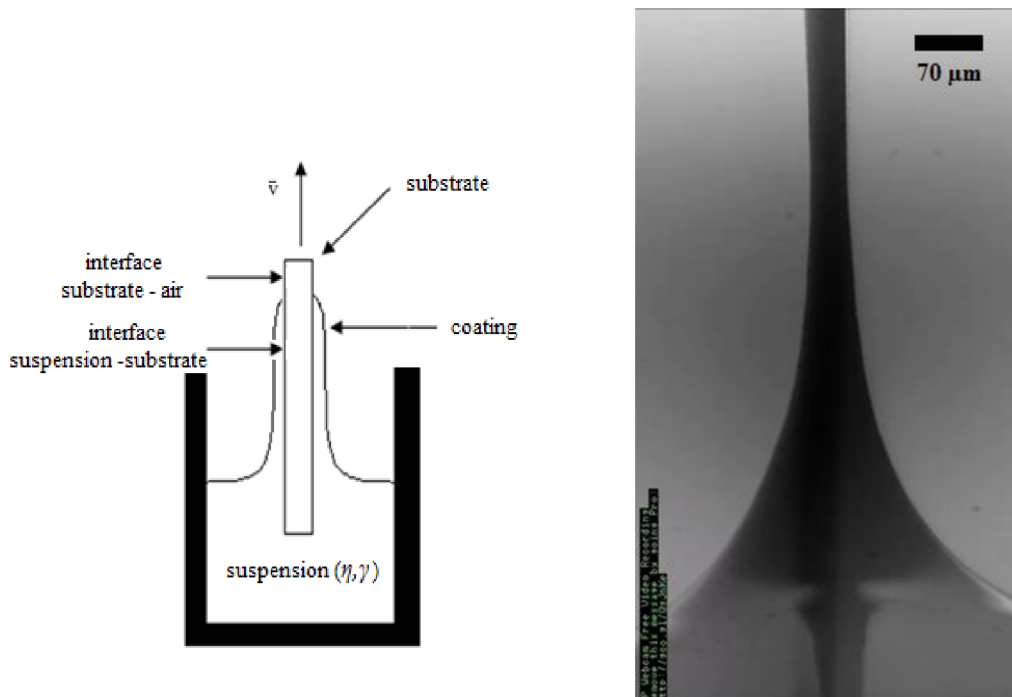
Figure 18. Schematic and real illustration of dip-coating.

3.6.2 LLD theory

One theory, which links the film thickness on the fiber and coating conditions, is the LLD theory that processed Landau and Levich Deryagin. LDD theory determines the thickness of the coating as a result of viscous, capillary, gravitational and inertial forces. To describe the results of these forces auxiliary numbers are used: capillary number, Bond number and Weber number. These numbers help to determine conditions of the coating and decisive forces for a layer formation [34].

3.6.3 Influence of viscosity, surface tension and rate of withdrawal

When the template is withdrawn from the suspension, creates two interfaces. The first interface is fiber-suspension and the second is air-suspension. At the first interface (fiber-suspension) acting viscous force due to presence of shear forces τ. This describes Newton's law of viscosity (Eq. 3.2) and due these forces suspension is captured on the surface of the fibers. Equitation (3.2) also shows that with increasing dynamic viscosity and withdrawal rate grow these shearing forces [34].

Conversely, at the interface of the slurry is critical growing meniscus, which is generated by withdrawing the fiber from the slurry, which is greater the greater the film layer is formed on the fiber. Against this acts surface tension which prevents increasing surface interface [34].

From these findings can be concluded, that the rate of withdrawal and viscosity helps form the film while the surface tension has the opposite effect. It is obtained the first parameter, the capillary number, which is defined as follows [34]:

$$Ca = \frac{\eta v}{\gamma},$$ (3.6)

where: η = viscosity,   [Pa × s]

                 v = rate of withdrawal,   [m × s^{-1}]

                 γ = surface tension.   [J × m^{-2}]

With increasing capillary number starts at a certain stage the layer to grow more than would be expected, which means that coating begin to have a greater impact inertia forces. This gives us Weber describes the number that relates the forces of inertia (ρv^2) and capillary forces (r/γ). Weber number is defined as follows [34]:

$$We = \frac{\rho v^2 \eta}{\gamma}, \qquad\qquad\qquad\qquad\qquad (3.7)$$

where: ρ = density,   [kg × m^{-3}]

               v = rate of withdrawal,   [m × s^{-1}]

               η = viscosity,   [Pa × s]

               γ = surface tension.   [J × m^{-2}]

Another factor which has not been mentioned is the influence of gravity to the coating process. It is necessary to decide whether or not they can be neglected. Capillary length (κ^{-1}) is defined as the comparison of Laplace and hydrostatic pressure in the liquid. Capillary length is defined as follows [34]:

$$\kappa^{-1} = \sqrt{\frac{\gamma}{\rho g}}, \qquad\qquad\qquad\qquad\qquad (3.8)$$

where: γ = surface tension,   [J × m^{-2}]

               ρ = density,   [kg × m^{-3}]

               g = acceleration of gravity.   [m × s^{-2}]

Gravity can be ignored if $r < \kappa^{-}$. This condition is based last auxiliary number, which helps determine the mode of coating is Bond number. Bond number is defined as follows [34]:

$$Bo = \frac{\rho g r^2}{\gamma}, \qquad\qquad\qquad\qquad\qquad (3.9)$$

where: ρ = density,   [kg × m^{-3}]

               g = acceleration of gravity,   [m × s^{-1}]

               r = diameter of fiber,   [m]

               γ = surface tension.   [J × m^{-2}]

3.6.4   Coating modes

The above auxiliary numbers (Ca, We, Bo) help to determine coating mode in which is under the given conditions (viscosity and surface tension of suspension, rate of withdrawal fiber) dip-coating process. Various modes are differentiated by the forces under the given conditions prevail. These modes are called visco-capillary, visco-inertial and boundary layer mode. In each of these modes leads to different changes of thickness depending on the capillary number. This is shown in Figure 19.
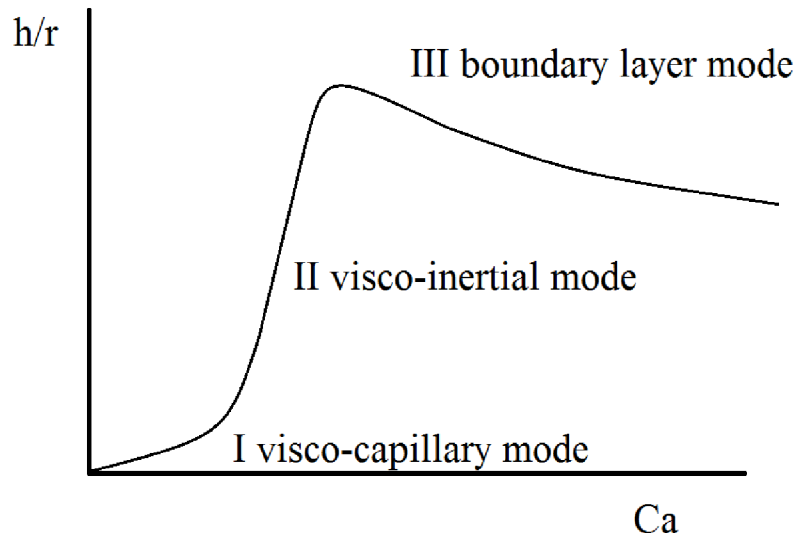
Figure 19. Dependence of the ratio of thickness and radius of the fibers to the capillary number [34].

Visco-capillary mode

Visco-capillary mode takes place at low speeds and viscosities, possibly under high surface tension. Capillary and Weber number are low and the main forces acting are viscous and capillary forces. In this mode, it can be observed only a relatively small increase of thickness due to the increase capillary number. The coating thickness can be expressed by the equation 3.10 [34]:

$$h = 1.34 r Ca^{2/3},\tag{3.10}$$

where: h = thickness,   [m]

    r = diameter,   [m]

    Ca = capillary number.   [-]

This simple relationship is only valid if $r \gg h$. If the conditions are not met, White and Tallmage correction have to be used. That reflects when thickness of film and diameter of fiber are similar. White and Tallmage correction is expressed in equation 3.11 [34]:

$$h = \frac{1.34 r Ca^{2/3}}{1 - 1.34 r Ca^{2/3}},\tag{3.11}$$

where: h = thickness,   [m]

    r = diameter,   [m]

    Ca = capillary number.   [-]

Bond number characterized the gravitational force, when Bond number is close to zero the gravitational force can´t be neglected, the entrainment law for the thickness of the coated layer is expressed in equation 3.12 [34]:

$$h = 0.94\kappa^{-1}Ca^{2/3},$$
(3.12)

where: h = thickness,   [m]

          κ^{-1} = diameter,   [m]

          Ca = capillary number.   [-]

Visco-inertial mode

Conditions for visco-inertial mode are after reaching of certain withdrawal rate and the film begins to significantly grow on the template (see Figure 19, part II). The increase of the thickness is much larger than would be expected based on the increase of the capillary number due the higher coating velocity. To understand the sharp increase in the film thickness the influence of inertial forces need to be considered. Inertial forces entrain them more material from the suspension and capillary forces and capillary forces become less important. Condition for this mode is that the Weber number approaching 1. The coating thickness in this mode can be expressed by the equation 3.13 [34]:

$$h = \frac{1.34rCa^{2/3}}{1-We},$$
(3.13)

where: h = thickness,   [m]

          r = diameter,   [m]

          Ca = capillary number,   [-]

          We = Weber number.   [-]

Boundary layer mode

Conditions for boundary layer mode are at high withdrawal rate. If Weber number goes to one, the thickness is determined by viscous, capillary and inertial forces, if rate of withdrawal is further increased and the Weber number is larger than one, the capillary forces can be ignored and only the viscous and inertial forces need to be considered. There was no further significant increase of thickness and due to the high rate of withdrawal must also include a length of reservoirs. Law for the thickness of the coated layer in this mode is expressed in equation 3.14 [34]:

$$h = 1.2\sqrt{\frac{\eta L}{\rho v}},\qquad\qquad\qquad\qquad\qquad\qquad\qquad\qquad\text{(3.14)}$$

where: h = thickness, [m]

η = viscosity, [Pa × s]

L = length of reservoirs, [m]

ρ = density, [kg × m^{-3}]

v = rate of withdrawal. [m × s^{-1}]

Overview of these modes are shown in Table 5:

Table 5. Overview laws and exceptions for the different coatings modes [34].

Mode	Name	Rate of withdrawal	Validity	Forces	Thickness
	Visco-capillary	Low	Ca<0,64 We<1	viscous capillary	$h = 1.34rCa^{2/3}$
I	Visco-capillary with White and Tallmage corection	Low	Ca<0,64 We<1 r ≈ h	viscous capillary	$h = \dfrac{1.34rCa^{2/3}}{1 - 1.34rCa^{2/3}}$
	Visco-capillary when gravity can´t be ignored	Low	Bo>1 We<1	viscous capillary gravita-tional	$h = 0.94\kappa^{-1}Ca^{2/3}$
II	Visco-inertial	Medium	We→1	viscous capillary inertial	$h = \dfrac{1.34rCa^{2/3}}{1 - We}$
III	Boundary layer	High	We>1	viscous inertial	$h = 1.2\sqrt{\dfrac{\eta L}{\rho v}}$

4 EXPERIMENTAL PROCEDURE

4.1 Materials

In the preparation of thin wall ceramic hollow fibers by dip-coating we have two essential input materials: suspensions and fibers. The fiber serves as a sacrificial template and suspensions as coating which is applied on the template. In this chapter suspensions and fibers will be characterized.

4.1.1 Suspensions

In this work two types of suspension are used, hydroxyapatite suspension and titania suspension. Their preparation is in many respects similar, but because of the fundamental differences between produced powders differences in preparation and proportions of raw materials. This part will be described feedstock, particularly ceramic powders, for the preparation of a suspension preparation itself will be described in the next chapter.

Hydroxyapatite suspensions

The basis of this suspension is commercially available hydroxyapatite powder $Ca_5(OH)(PO_4)_3$ having a purity p.a. (for analysis) and the contents of main components ≥ 90 %, from Sigma Aldrich. This powder was subsequently calcined at 800 °C due to the high activity of bacteria which caused a very low durability of suspension. As dispersant was used Dolapix CE64, which was used to stabilize the suspension. Methylcellulose with a defined viscosity of 15 cP was used as a binder. For pH adjustment were used 25% ammonia solution.

Titania suspensions

The basis of this suspension is commercially available TiO_2 nanopowder with a particle size having < 25 nm and the contents of main components ≥ 97 %, from Sigma Aldrich. As a dispersant was used Dolapix CE64 and as a binder methylcellulose 15 cP. For pH adjustment in this case was due to different starting powder was used molecular phosphoric acid solution.

4.1.2 Sacrificial templates

Fiber serves as a template, which is in the course of the experiment coated and subsequently high temperature sacrifice. For dip-coating are important mechanical properties, the number and surface of filaments and diameter of fiber. For the subsequent sintering regime are important temperatures of decomposition, thermal expansion and relaxation fibers at high temperatures. Three were selected UHMW PE, carbon and cotton fibers for this work.

UHMW PE fiber

This fiber is formed by a high molecular weight polyethylene has a diameter 35 μm and it has very good mechanical properties (mechanical strength in range of 1400-3000 MPa). It is formed of several interconnected filaments which are glued together by Teflon, it results in a poorly defined surface. Temperature of decomposition fiber is between 500-600 ℃. It has a large ratio of thermal expansion and high temperature leads to a considerable relaxation of fiber. UHMW PE fiber we can see in Figure 20.
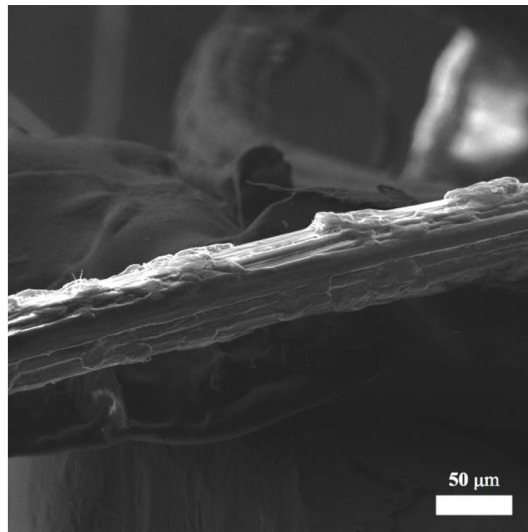
Figure 20. UHMW PE fiber used as sacrificial template, diameter 35 μm.

Carbon fiber

This fiber has diameter 34.5 ± 2.5 μm and it has relatively good mechanical properties (mechanical strength 860 MPa), but shear strength is low relative to the fiber diameter. It is formed of a monofilament carbon with a definable surface. Temperature of decomposition is between 400-450 ℃. It has a very small thermal expansion and high temperatures leads to minimal relaxation of fiber. Carbon fiber is shown in Figure 21.
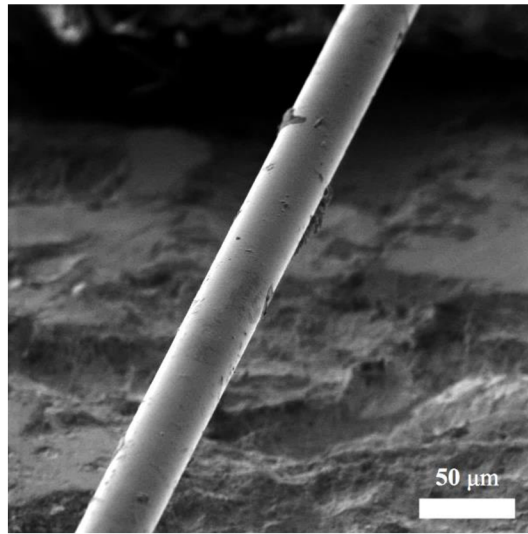
Figure 21. Carbon fiber used as sacrificial template, diameter 34.5 ± 2.5 μm.

Cotton fiber

This fiber has diameter about 170 μm and it has good mechanical properties (mechanical strength in range of 400-800 MPa). It is formed of loosely braided filaments of cotton, it results in a poorly defined surface and free spaces between the filaments. Temperature of decomposition is between 450-550 °C. It has a small thermal expansion and high temperatures leads to small relaxation of fiber. Cotton fiber can be seen in Figure 22.
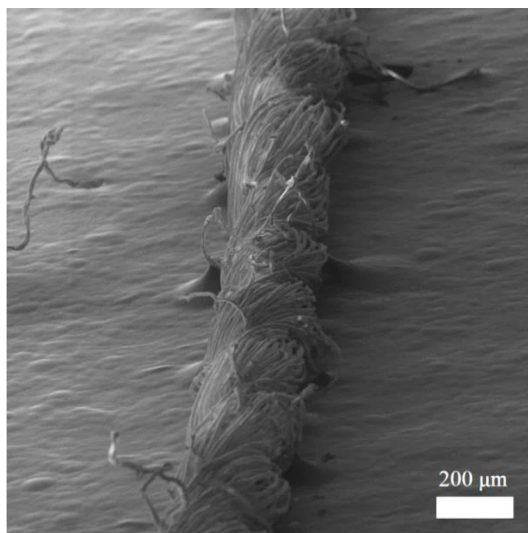
Figure 22. Cotton fiber used as sacrificial template, diameter about 170 μm.

4.2 Production of suspensions

Due to the very similar process for the preparation of both types of suspension will be generally described preparation procedure and subsequently commented suspension specifics for hydroxyapatite and titania suspensions.

A given amount of water was heated to 80 °C and then added to methylcellulose. After dissolution was added dispersant and adjusted pH. To the resulting mixture was then gradually added ceramic powder. Then to the suspension were added ceramic balls and the suspension was placed on rotation mill for 24 hours. Milling need to be applied before each dip-coating at least 1 hour. If suspension contains large amount of air bubbles it is possible to add octanol, which reduces surface tension, but it can have a negative impact in the coating, which under certain conditions can result in drops instead of film.

Hydroxyapatite suspension

Hydroxyapatite suspensions were made in several variants.

The first series of suspensions 17HAP-XMC (where X expresses the content of methylcellulose) was designed for the coating of PE fibers, which are characterized by high thermal expansion and considerable relaxation of fiber. Therefore was used higher volume percentage of ceramic powder (17.5 vol. %) and various volume percentage of binder (1 - 3.5 vol. %). Suspensions were labeled according to the content of binder A-E, overview suspensions 17HAP-XMC series is shown in the Table 6. Hydroxyapatite suspensions are stable in alkaline environments and therefore pH was adjustment by 25% ammonia solution.

The exact compositions of the suspensions with the lowest and highest content are binder shown in Table 7 and Table 8.

Table 6. Content of binder series 17HAP-XMC.

17HAP	A	B	C	D	E
vol.% binder (X)	1	1.5	2	3	3.5

Table 7. Hydroxyapatite suspension 17HAP-1MC.

Weight [g]	Volume [cm³]	Chemical	Function	Density [gcm⁻³]	Weight [%]	Volume [%]
189.52	189.52	Water	Solvent	1.00	57.83%	80.01%
2.03	1.69	Dolapix CE64	Dispersant	1.20	0.62%	0.71%
131.06	41.48	Calcined HAP powder	Ceramic powder	3.16	39.99%	17.51%
3.02	2.32	Methylcellulose 15 cP	Binder	1.3	0.92%	0.98%
6 drops		Octanol	Surfactant			
2.09	1.88	Amoniac (25%)	Stabilizer	1.11	0.64%	0.79%

Table 8. Hydroxyapatite suspension 17HAP-3.5MC.

Weight [g]	Volume [cm³]	Chemical	Function	Density [gcm⁻³]	Weight [%]	Volume [%]
183.51	183.51	Water	Solvent	1.00	55.66%	77.43%
2.24	1.87	Dolapix CE64	Dispersant	1.20	0.68%	0.79%
131.13	41.50	Calcined HAP powder	Ceramic powder	3.16	39.77%	17.51%
10.77	8.28	Methylcellulose 15 cP	Binder	1.3	3.27%	3.50%
6 drops	6 drops	Octanol	Surfactant			
2.04	1.83	Amoniac (25%)	Stabilizer	1.11	0.62%	0.77%

The hydroxyapatite suspension 15HAP-3MC was used for coating the cotton fiber, because the fiber has not so high thermal expansion and relaxation at high temperature as PE fibers. Therefore it was possible to use a smaller volume percentage of the ceramic powder (15 vol. %) and larger amount of binder (4 vol. %). The exact composition of the suspension 15HAP-3MC shown in Table 9.

Table 9. Hydroxyapatite suspension 15HAP-3MC.

Weight [g]	Volume [cm³]	Chemical	Function	Density [g/cm3]	Weight [%]	Volume [%]
200.03	200.03	Water	Solvent	1.00	59.23%	79.29%
2.50	2.08	Dolapix CE64	Dispersant	1.20	0.74%	0.83%
119.55	37.83	Calcined HAP powder	Ceramic powder	3.16	35.40%	15.00%
13.12	10.09	Methylcellulose 15 cP	Binder	1.3	3.89%	4.00%
10 drops	10 drops	Octanol	Surfactant			
2.50	2.25	Amoniac (25%)	Stabilizer	1.11	0.74%	0.89%

Titania suspension

Titania suspension 10TiO2-1MC was used for coating of the carbon fiber, it was therefore not necessary to count with thermal expansion or relaxation at high temperature. Smaller particle size of the powder only enables to reach smaller volume percentage of titania in suspesion(10 vol. %) compare with HAP suspensions. Advantage of the fiber is possibility to use only small amount of binder (1 vol. %). Hydroxyapatite suspensions are stable in acid environments and therefore pH was adjustment by phosphoric acid solution. The exact composition of the suspension 10TiO2-1MC shown in Table 10.

Table 10. Titania suspension 10TiO2-1MC.

Weight [g]	Volume [cm³]	Chemical	Function	Density [g/cm3]	Weight [%]	Volume [%]
161.07	161.07	Water	Solvent	1.00	66.16%	88.08%
1.94	1.62	Dolapix CE64	Dispersant	1.20	0.80%	0.89%
78.02	18.32	TiO_2 powder	Ceramic powder	4.26	32.05%	10.02%
2.42	1.86	Methylcellulose 15 cP	Binder	1.30	1.00%	1.02%
150 drops		H_3PO_4 1M	Stabilizer	1.11		0.00%

4.3 Viscosity of suspensions

For the 17HAP-XMC series, the viscosity was measured to determine the effect of viscosity on the shape stability. The viscosity was measured using a rotary viscometer (Digital rotary viscosimeter 807/1, Nahita, Spain). The viscosity was measured at temperature 22 ℃.

4.4 Dip-coating

The coating process was performed on a device specially developed at BUT for coating thin fibers. This device allows the coating of these fibers for various speeds. It can operate in two settings, continuous and semi-continuous. The continuum setting is used to coat fibers of great length, the fiber is at the bottom of apparatus are wound on the coil and then goes through the slurry tank, the fiber is withdrawn from the suspension at a given speed and then passes through the drying chamber and the winding system is again wound onto the coil. Semi-continuous setting is used for testing the fibers of short lengths of fiber is pulled through the PE tube tipped funnel, tube with the fiber is then filled with suspension and the fiber is withdrawn from the suspension at a given speed. This setting do not allow use a drying chamber. The test fibers were coated with a suspension and withdraw speed 5-35 cm $\times$ s^{-1}, using both settings. The whole process was optical observed to measure the diameter of the coating before drying. Dip-coater shown is in Figure 23.
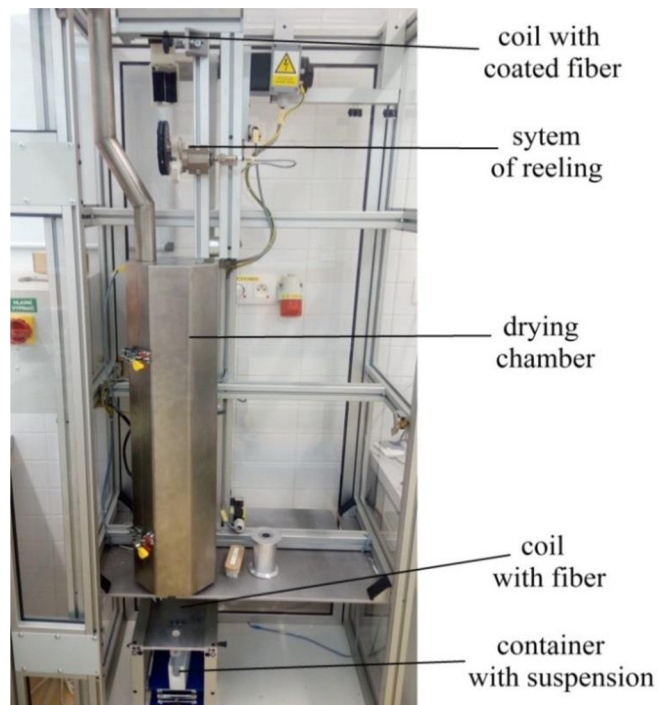
Figure 23. Dip-coater, device specially developed at BUT for coating thin fibers. It can operate in two settings, continuous and semi-continuous.

4.5 Sintering

After drying and cut to the appropriate length of the fiber, these fibers were placed on alumina plate and sintered in a resistance furnace. Hydroxyapatite hollow fibres were sintered at 950 ℃, 1000 ℃, 1100 ℃, 1200 ℃. Titania hollow fibers were sintered at 700 ℃, 1200 ℃. These sintering cycles are shown in Figure 24.
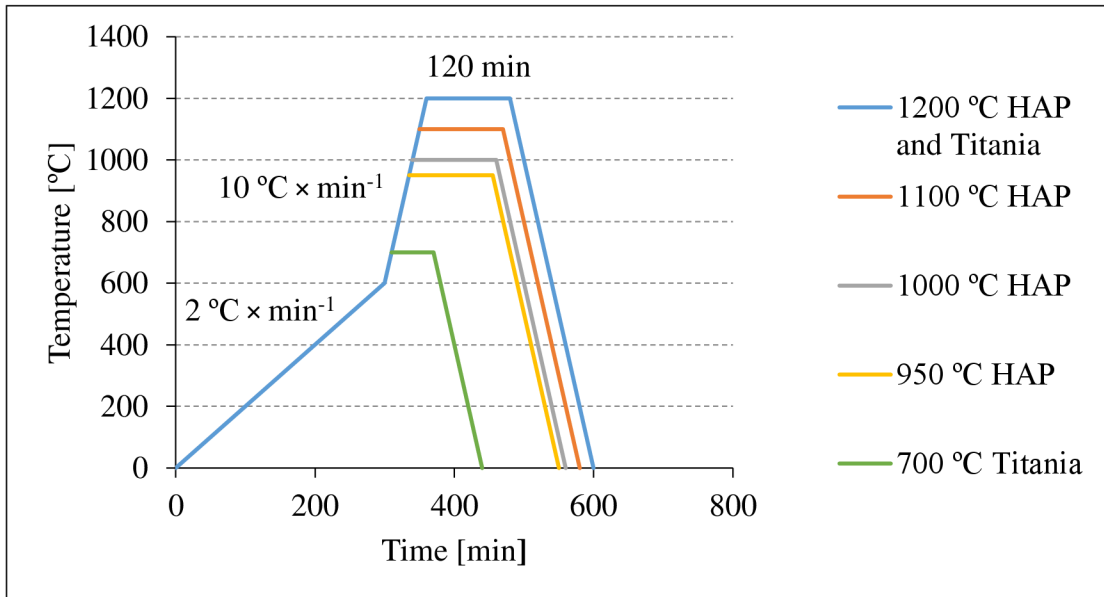
Figure 24. Sintering cycles in which the coated fibers were sintered. Realized in a resistance furnace

4.6 Analysis of the microstructure

Sintered samples were subsequently prepared for the observation on a scanning electron microscope (Focused Ion Beam/Scanning Electron Microscope LYRA3, Tescan, Czech Republic). Subsequently were measured grain size and porosity. For measuring the grain size was used the linear intercept method [35]. For measuring larger areas was used network segments, for measuring ceramic hollow fibers were used the line segment parallel to the axis of the fiber. Both cases are shown in Figure 25.
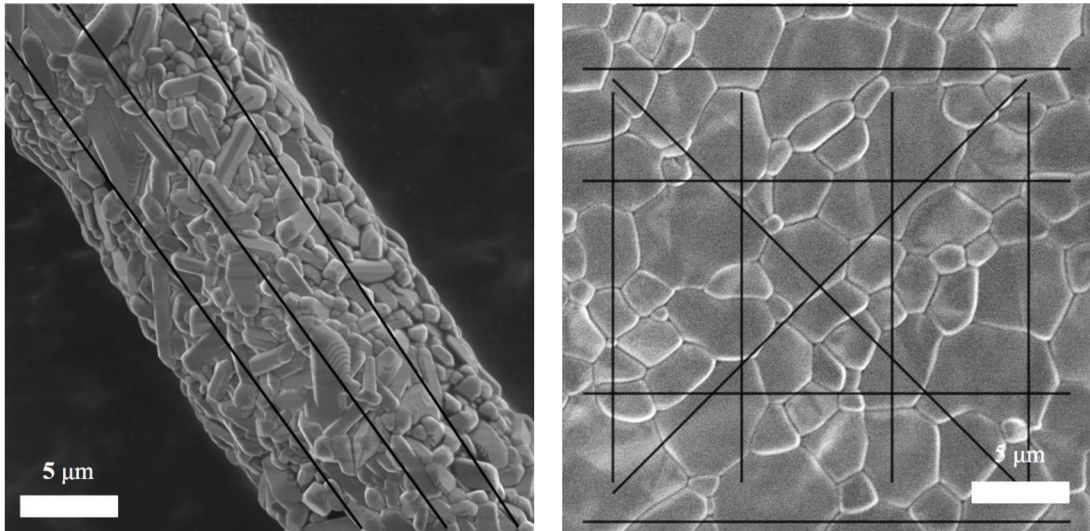
a) Example of titania hollow fiber measurement.

b) Example large surface of titania block measurement.

Figure 25. An example of the grain size measurement difference between ceramic hollow fibers (segment parallel to the axis) and large surfaces (network segments)

Porosity measurements conducted using thresholding images from electron microscopy, as shown in Figure 26.
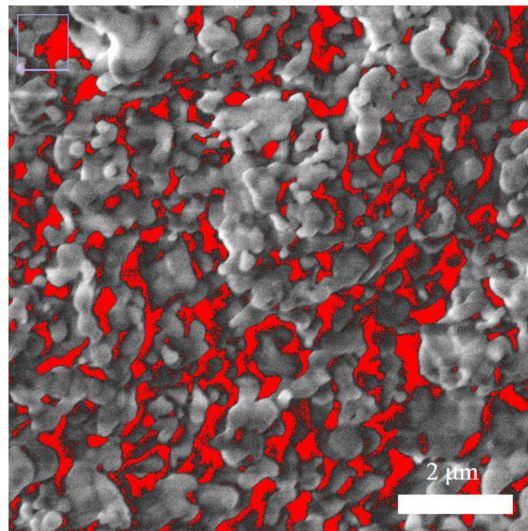
Figure 26. Example of sample for measurement of porosity plotted with the program ImageJ.

4.7 Biological testing

Biological tests were conducted in cooperation with Mendel University. Hydroxyapatite samples were cut and placed into a plastic composition specially treated for the biological tests. They were fixed to the edge by a solution of methyl cellulose. These samples were subsequently tested at Mendel University in culture n-myc amplified neuroblastomas. Different concentrations of cells were seeding on the hydroxyapatite hollow fiber and subsequently monitored using light and fluorescence microscopy. The beginning and center of the ceramic hollow fiber also free cells and response cells with adhesive were monitored.

5   RESULTS

5.1   Ceramic thin fibers from hydroxyapatite

5.1.1   Properties of HAP suspensions

Viscosity measurements were performed on a 17HAP-XMC (X is volume percent of methylcellulose - MC) series where the different viscosity was caused by different content of methylcellulose. The measurement results are shown in the Figure 27. It is evident that the viscosity of the suspension increases with the increasing content of methylcellulose. It is also apparent that the viscosity is stabilized at an increasing shear rate (speed).
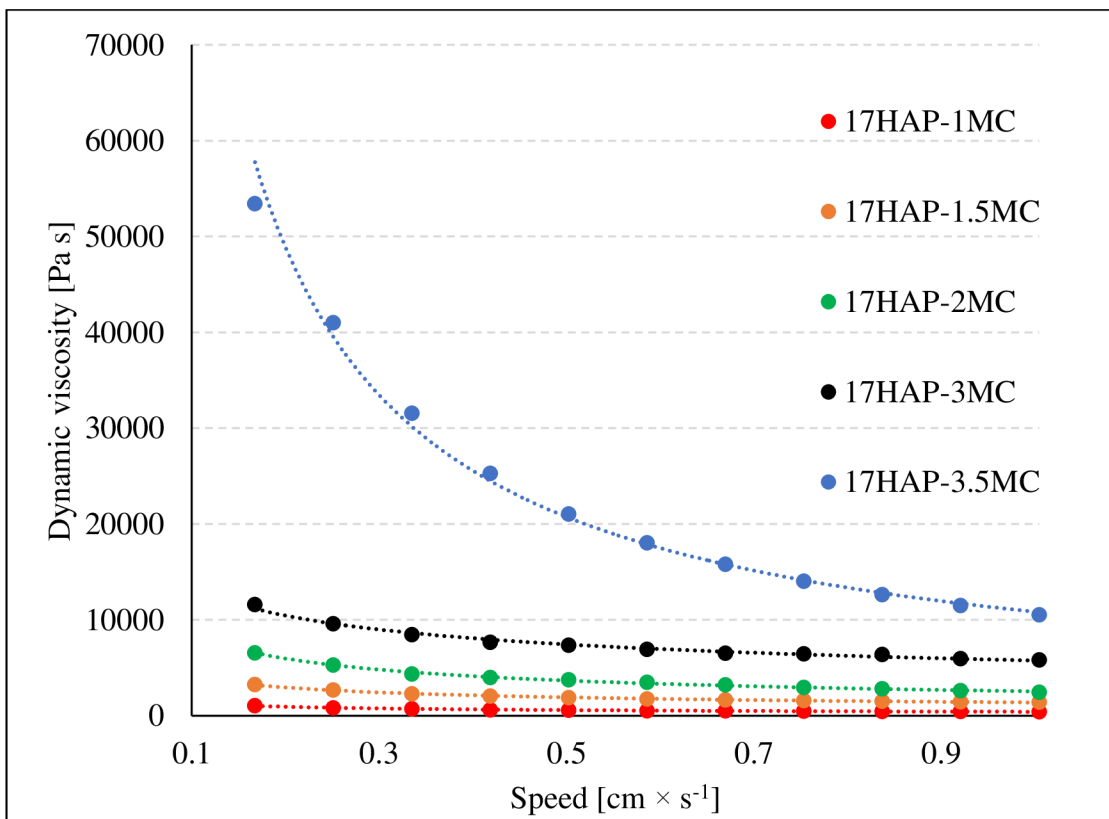
Figure 27. Dependence of dynamic viscosity on rotation speed of the cylinder.

5.1.2   Shape stability on various templates

UHMW PE fiber

UHMW PE fibers were coated with a series of suspensions 17HAP-XMC (X is volume percent of MC). Rate of withdrawal was between 5-35 cm $\times$ s^{-1}. Thanks to the very good mechanical properties of these fibers was possible use continuous and semi-continuous setting.

During the use of suspensions with lower content of methylcellulose (with lower viscosity) it was observed that the thickness of the film or drops is too small and structure collapse during the subsequent sintering process. At higher rates of withdrawal it was observed creating of droplet, above a certain critical speed, the film becomes unstable. This dependence is shown in Figure 28, where it was used the suspension 17HAP-1MC (with lower content of MC). Combinations of collapsed structure and drops are halfdrops.
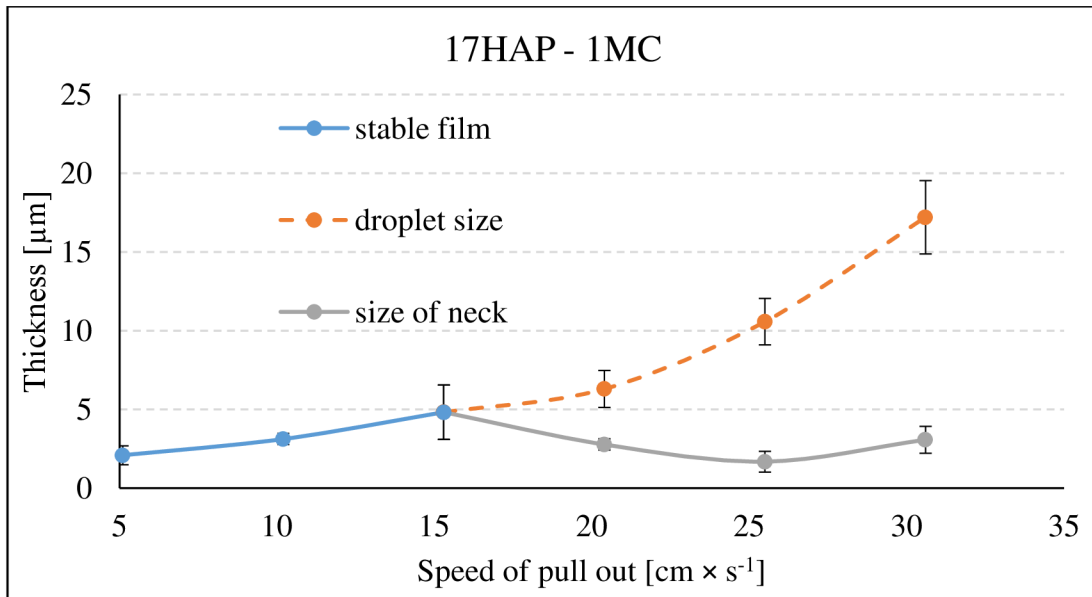
Figure 28. Film thickness dependency of the drawing rate, after exceeding the critical speed of formation of drops.

Summary of the resulting shapes after sintering are summarized in the Table 11. Demonstrations of shapes are shown in Figure 29.

Table 11. Summary of results after sintering for shape stability depending on the speed and viscosity of the suspension.

Rate of withdrawal (cm × s⁻¹)	5	10	15	20	25	30	35
17HAP-1MC	Collapsed	Collapsed	Collapsed	Collapsed	Collapsed	Halfdrops	Halfdrops
17HAP-1.5MC	Collapsed	Collapsed	Halfdrops	Not measured	Not measured	Not measured	Not measured
17HAP-2MC	Collapsed	Collapsed	Drops	Big drops	Not measured	Not measured	Not measured
17HAP-3MC	Big drops	Not measured	Not measured	Not measured	Not measured	Not measured	Not measured
17HAP-3.5MC	Film	Film	Film	Film	Film	Film	Film

| Collapsed. | Halfdrops. |

| Drops. | Film. |
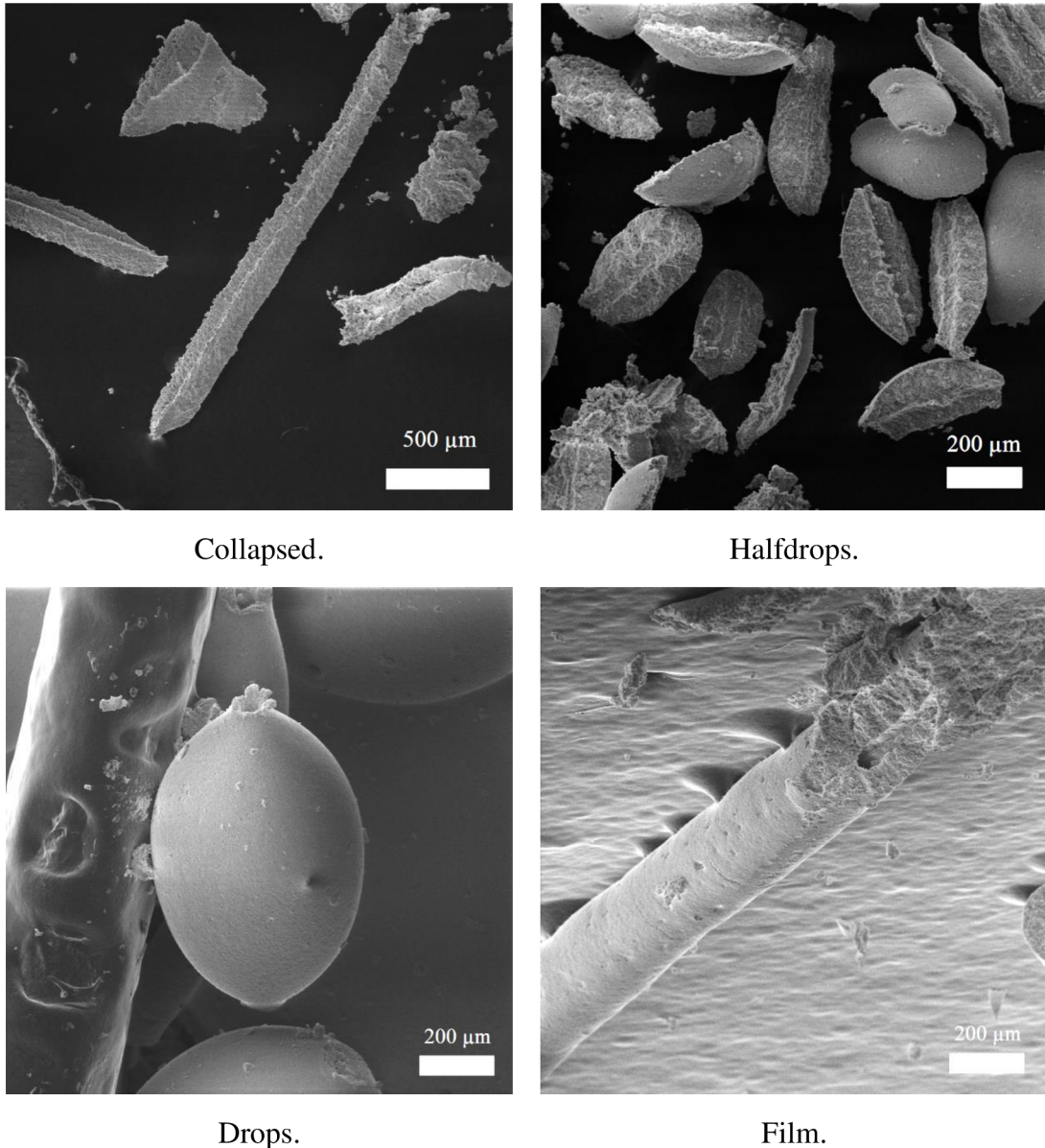
Figure 29. Examples of shapes after sintering of thin films produced by dip-coating UHMW PE fiber at various withdrawal rates and suspensions (17HAP-XMC), sintered at 950 °C (see Table 11).

Cotton fiber

Cotton fibers were coated with suspension 15HAP-3MC and with different rate of withdrawal. The cotton fiber does not have good mechanical properties, but because of its larger diameter it could be used for continuous and semi-continuous setting. When the cotton fiber was coated, the resulting structure was film only. If it has been coated without modification of fiber before coating after sintering there is no free channel but only the region of lower density material. Ceramic fiber with region of lower density material instead of channel is shown on Figure 30.
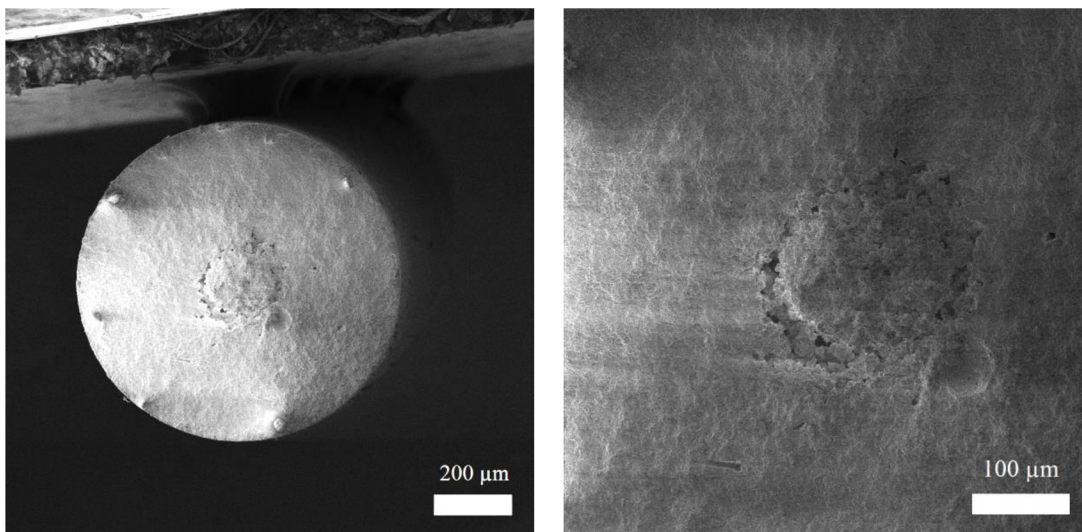
Figure 30. Ceramic fiber produced by dip-coating cotton fiber with hydroxyapatite (15HAP-3MC), fiber has not through channel just region with lower density material, sintered 950 ℃, rate of withdrawal 20 cm × s^{-1}.

However, if the fiber was coated with methylcellulose, ceramic fiber with a through channel is formed. The ceramic hollow fiber is shown in Figure 31.
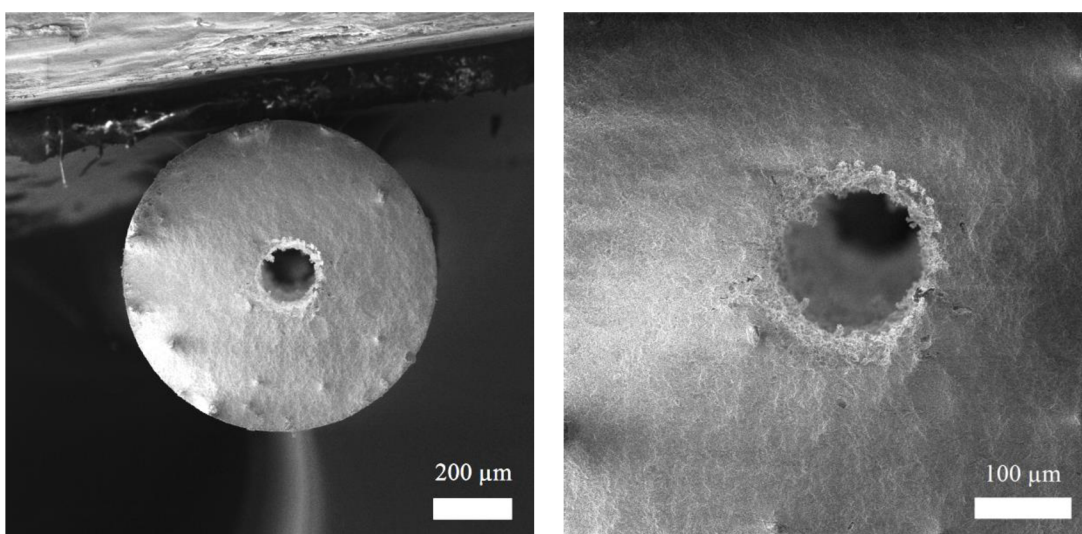
Figure 31. Ceramic fiber produced by coating cotton fiber made by pre-coating the cotton fiber with methylcellulose and then coating with hydroxyapatite (15HAP-3MC), fiber has through channel, sintered 950 ℃, rate of withdrawal 20 cm × s^{-1}.

Carbon fiber

Carbon fibers were coated with a series of suspensions 17HAP-1MC. Rate of withdrawal was between 5-35 cm × s^{-1}. When the carbon fiber was coated, the resulting structure was film or drops. The resulting ceramic hollow fibers can then

achieve very thin wall (1μm) without cracking the fibers. Ultrathin ceramic hollow fibers produced by coating carbon fibers are shown in Figure 32.
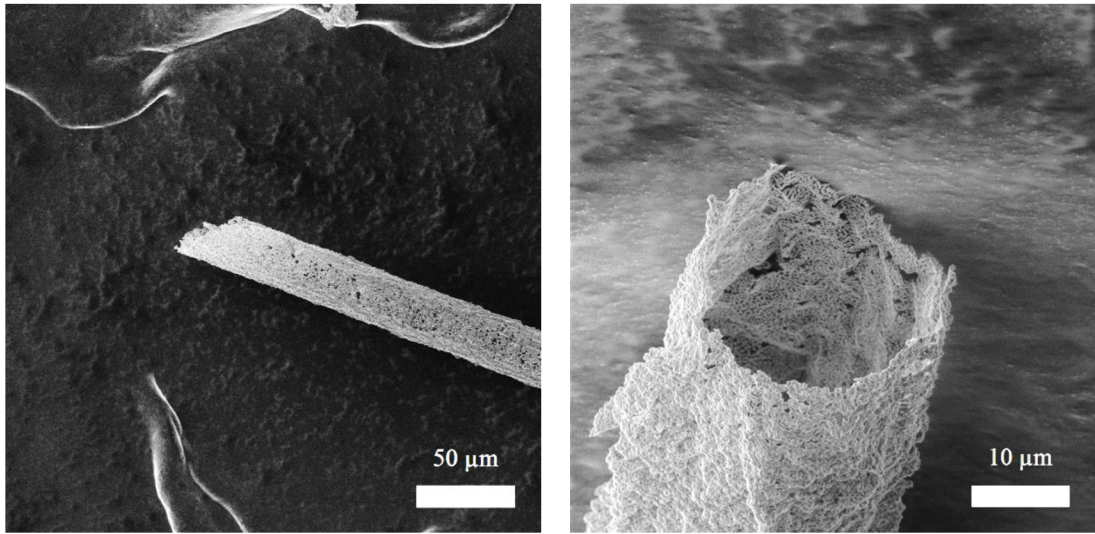
Figure 32. Ultrathin ceramic hollow fibers produced by dip-coating of carbon fibers with hydroxyapatite (17HAP-1MC), sintered 950 ℃, rate of withdrawal 5 cm × s^{-1}

5.1.3 Various thickness based on dip-coating process

For layer thickness measurement was selected UHMW PE fibers and suspension 17HAP-3.5MC to achieve a stable film across the range used rates of withdrawal. The film thickness was measured before drying immediately after coating by optical equipment.

The measurement results are summarized in the Table 12 and shown graphically in the Figure 33.

Table 12. Summary of results for the thickness measurement, depending on the rate of withdrawal (measured directly after coating before the drying procedure).

Rate of withdrawal [cm × s^{-1}]	5	10	15	20	25	30	35
Number of measurements [-]	10	10	10	10	10	10	10
Average wall thickness [μm]	5.4	29.1	36.9	46.6	53.8	54.9	53.0
Standard deviation [μm]	1.0	5.0	4.3	9.3	3.2	3.4	2.8
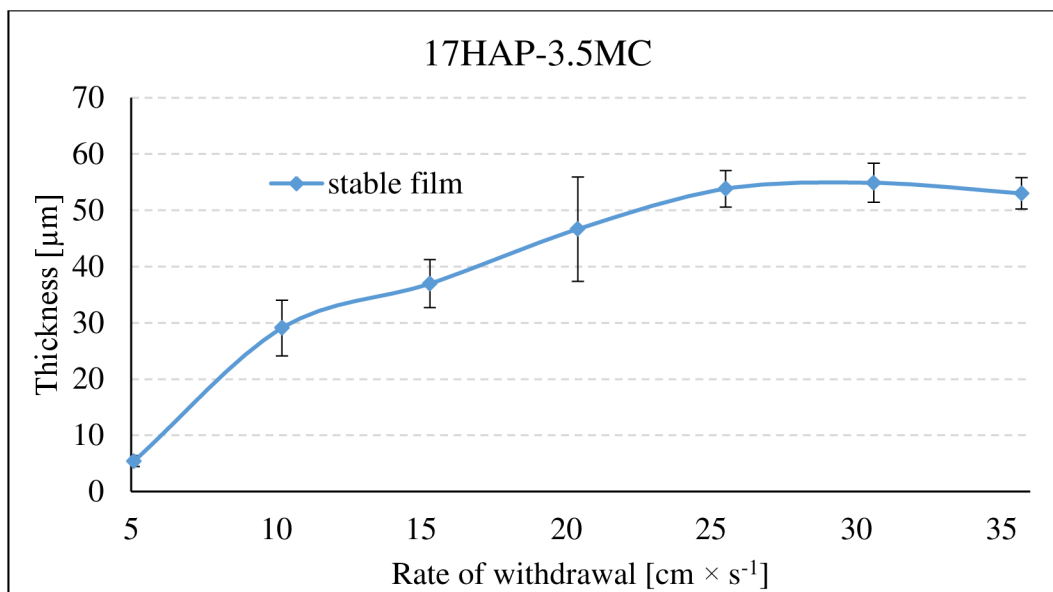
Figure 33. Dependence of thickness of the hydroxyapatite coating on various rates of withdrawal (5-35 cm $\times$ s^{-1}).

It is clear from the measured results that the thickness of the coating first grows rapidly, but it is subsequently settled or slightly decreasing.

5.1.4 The influence of sintering modes on grain size and porosity

For grain size and porosity measurement was selected cotton fibers and suspension 15HAP-3MC, thickness of the wall of these hollow ceramic fibers was approximately 300 μm. The samples were sintered at temperatures 950 ℃, 1000 ℃, 1100 ℃, 1200 ℃.

The measurement results are summarized in the Table 13 and shown graphically in the Figure 34 and Figure 35.

Table 13. Summary of results for grain size and porosity measurement, depending on the rate of withdrawal.

Temperature [ºC]	Grain size [μm]	Standard deviation of grain size [μm]	Number of grains intersected [-]	Porosity [%]	Standard deviation of porosity
950	0,3	0,02	986	18.4	0.8
1000	0,5	0,06	647	10.4	0.5
1100	0,7	0,09	489	6.2	0.6
1200	0,9	0,07	380	2.6	0.6
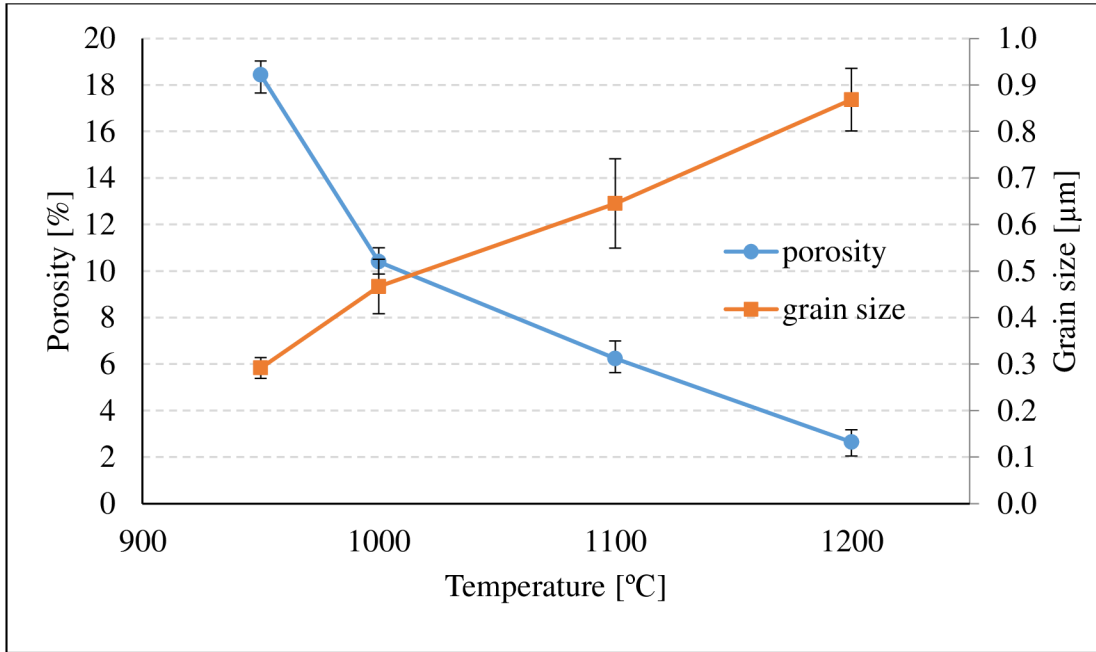
Figure 34. Dependence of grain size and porosity on temperature.

The measured results demonstrates that with the increasing sintering temperature increases the grain size and decreases the porosity. Illustrative demonstration of microstructures at sintered at various temperatures is shown on Figure 36.
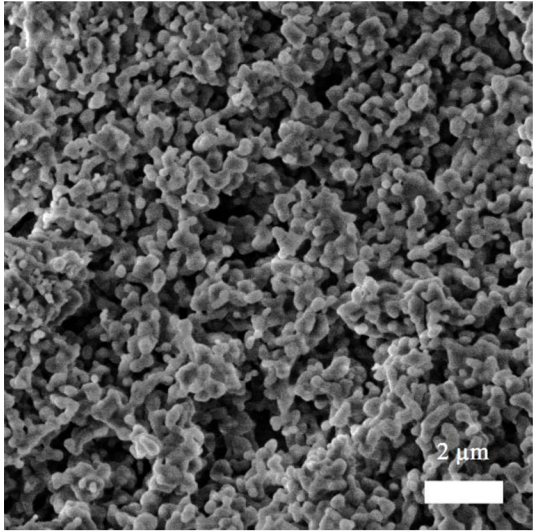
| sintered at 950 ℃ ℃ | sintered at 1000 ℃ |
| sintered at 1100 ℃ | sintered at 1200 ℃ |
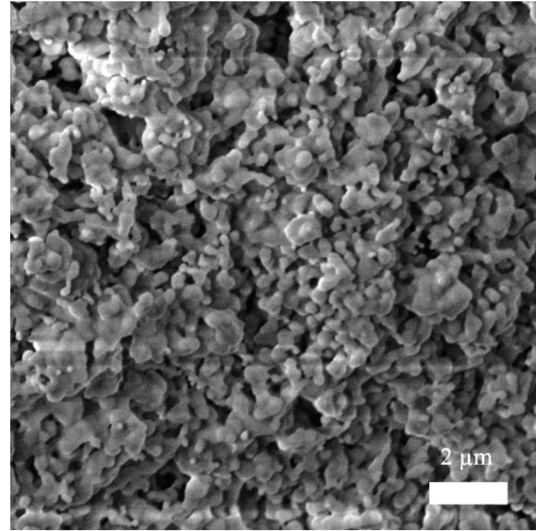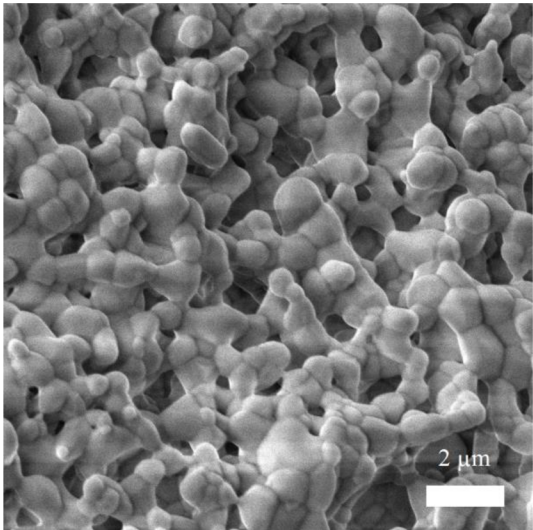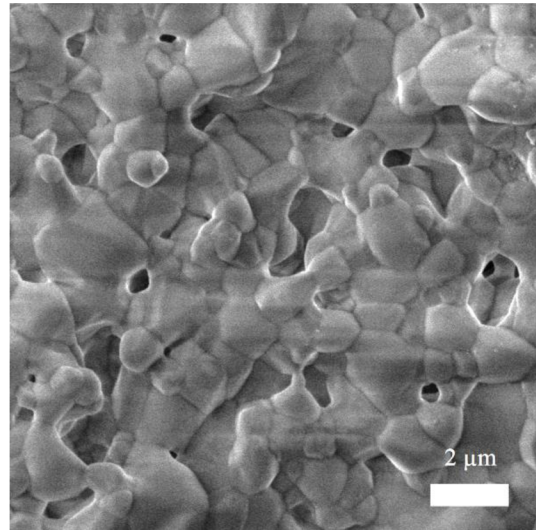
Figure 35. Examples of microstructure ceramic hollow fibers produced by dip-coating cotton fiber with hydroxyapatite (15HAP-3MC) at different sintering temperatures, rate of withdrawal 20 cm $\times$ s^{-1}.

5.1.5   Biological testing of porous HAP ceramic hollow fibers

Porous and hollow fiber for biological testing was prepared from UHMW PE fiber and suspension 17HAP-3.5MC by coating and sintering at 950 °C to achieve porous structure. Resulting ceramic hollow fibers had wall thickness after coating in the range of 30-50 μm. Monitoring parameters were adherence of the cells to the hollow fibers and the toxicity of the adhesives. The results of these biologic tests are shown in the Figure 36.
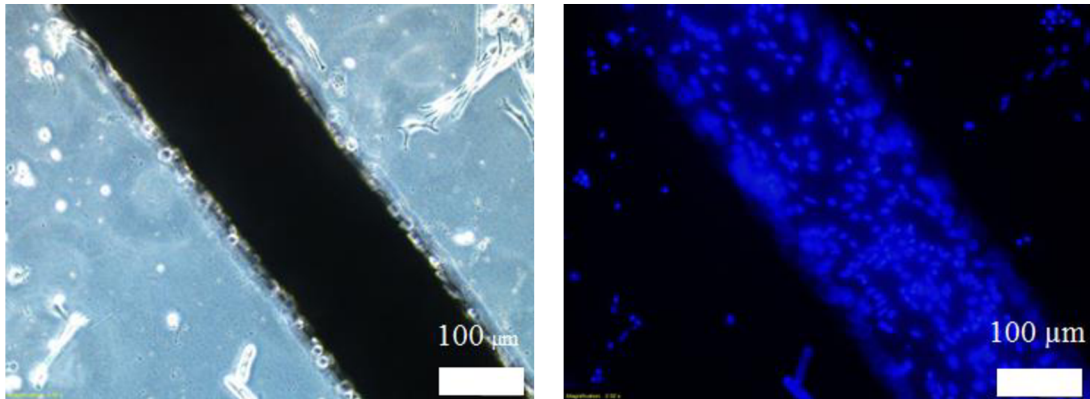
HAP samples observed by light
microscopy

HAP samples observed by fluorescence
microscopy

Figure 36. Biological testing of porous hollow fibers produced by dip-coating UHMW PE fiber with hydroxyapatite (17HAP-3.5MC) with outer diameter over 100 μm, sintered at 950 °C, rate of withdrawal 25 cm × s^{-1}.

Biological tests show that cells adhere to hydroxyapatite without difficulty and proliferate more efficiently than they do in the vicinity.

5.2   Ceramic thin hollow fibers from titania

5.2.1   Porous TiO$_2$ hollow fibers sintered at low temperatures

For low temperature sintering was selected carbon fibers and suspension 10TiO2-1MC, to achieve very low wall thicknesses. Low temperatures (700 °C) lead to a very porous structure with very fine grains. TiO$_2$ structures sintered at low temperatures is shown in Figure 37.
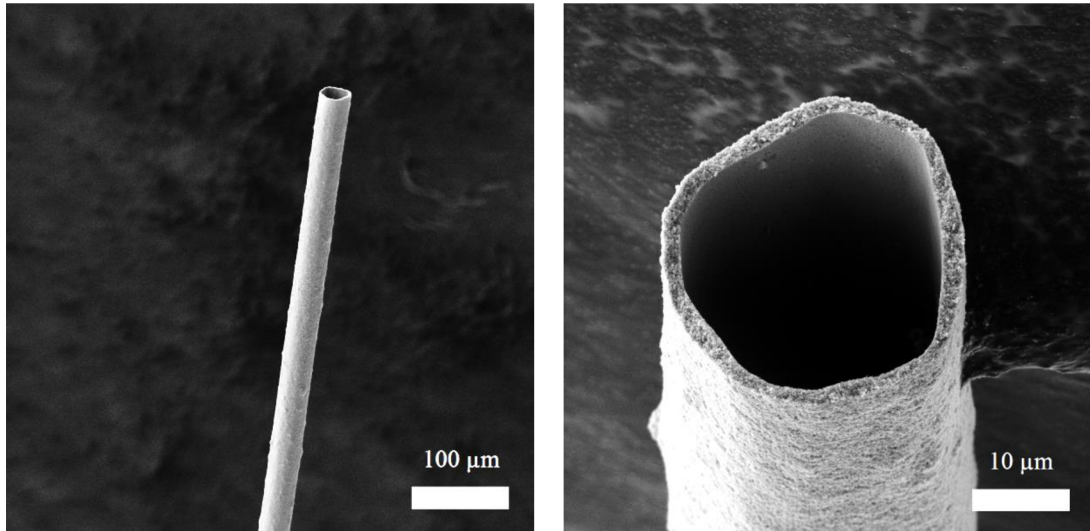
Titania ultrathin hollow fiber   Cross section of ultrathin hollow fiber

Figure 37. Examples of titania ultrathin hollow fiber produced by dip-coating
carbon fiber with titania (10TiO2-1MC), sintered at 700 ℃,
rate of withdrawal 5 cm $\times$ s^{-1}.

The phenomenon of increased concentration of material on the surface was also
observed on samples sintered at low temperature. This is shown on Figure 38 when
dense areas are visible close to the both surfaces (inner and outer), see the
"Microstructure of the hollow fiber wall cross section".

Microstructure of the hollow fiber   Microstructure of the hollow fiber wall
outer surface   cross section

Figure 38. Example of microstructures on surface and in cross section,
sintered at 700 ℃, rate of withdrawal 5 cm $\times$ s^{-1}.

5.2.2 Dense TiO$_2$ hollow fibers-grain size

For grain size measurement was selected carbon fibers and suspension 10TiO2-1MC, to achieve very low wall thicknesses. The samples were sintered at temperature 1200 °C. Subsequently, an analysis of the grain size dependence on wall thickness after sintering was performed. For comparison was subsequently cast block from the same suspension. It was dried and then sintered under the same conditions. Subsequently, the structure was analysed on the surface of a sintered sample and its core.

The measurement results are summarized in the Table 14 and grain size dependence on the wall thickness of ceramic hollow fiber is shown graphically in the Figure 39.

Table 14. Summary of results for wall thickness of ceramic hollow fiber and grain size measurement; internal diameter was 12.7 ± 0.5 µm.

Wall thickness [µm]	Wall thickness standart deviation [µm]	Grain size [µm]	Grain size standart deviation [µm]	Mumber of grain intersected [-]
0.6	0.3	1.1	0.1	452
2.0	0.5	1.3	0.3	85
3.5	1.4	1.5	0.2	629
18.8	0.4	1.6	0.1	418
21.1	1.0	1.9	0.2	224
21.3	0.9	2.1	0.3	436
Surface		2.7	0.6	418
Core		1.8	0.2	557
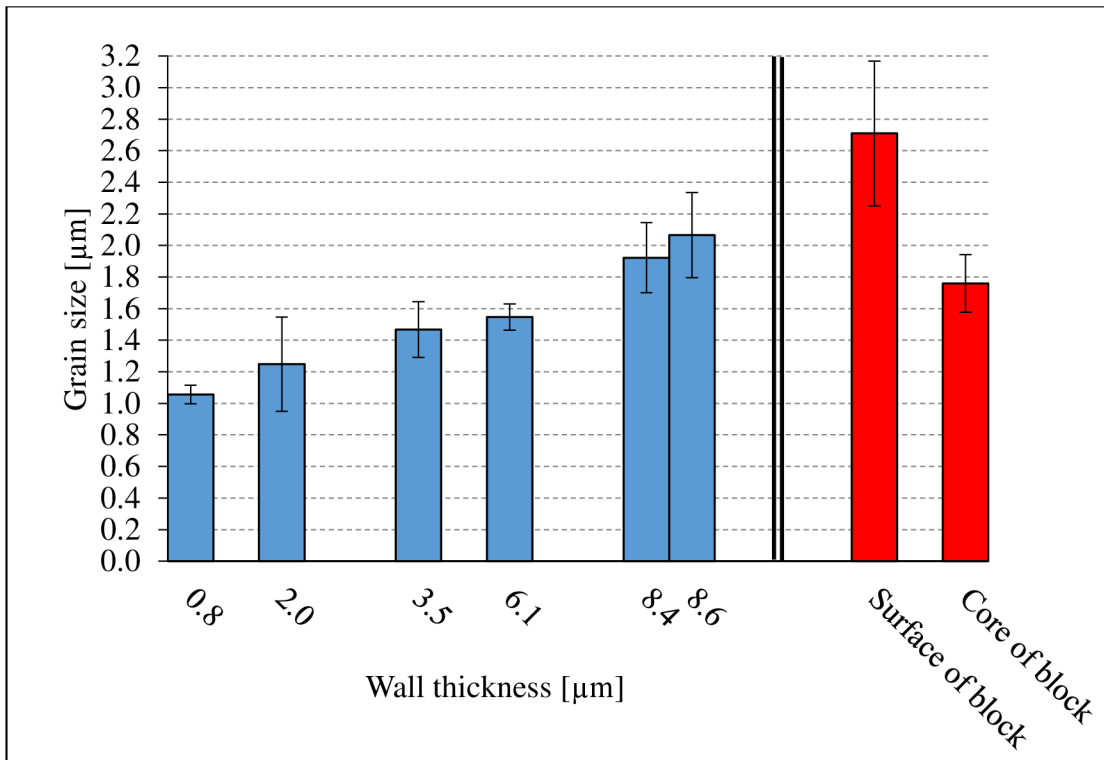
Figure 39. Dependence of grain size and wall thickness of titania hollow fiber sintered at 1200 ℃ and comparison with casted block surface and core sintered at same temperature.

The different microstructure of the cast sample on the surface and in the core can be seen in the Figure 40. An example of observed grain sizes of ultrathin ceramic fibers can be seen in the Figure 41.

Surface of block   Core of block
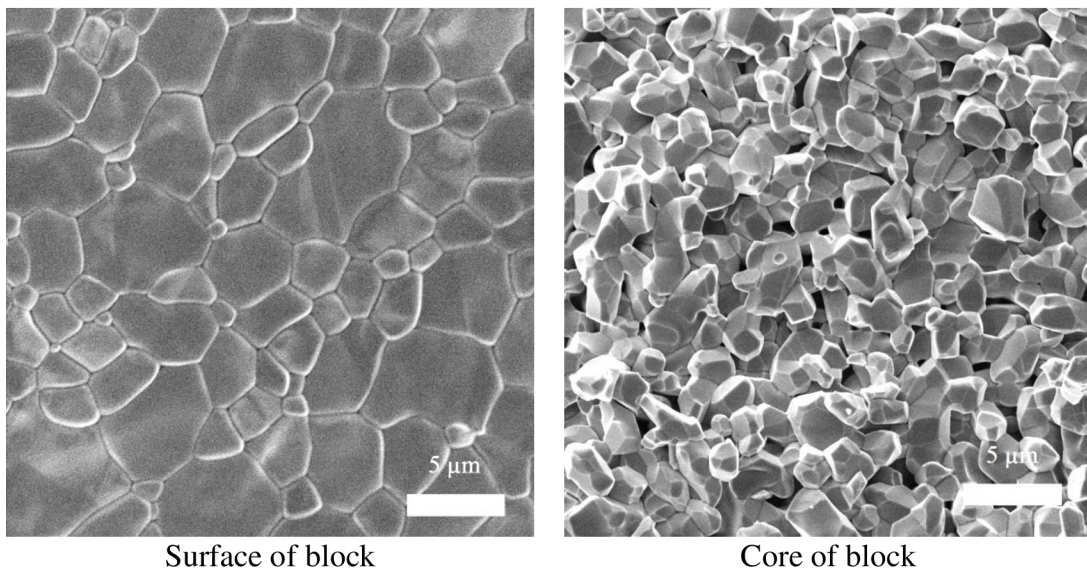
Figure 40. Example of microstructure titania (10TiO2-1MC) cast block on the surface and in the core, sintered at 1200 ℃.
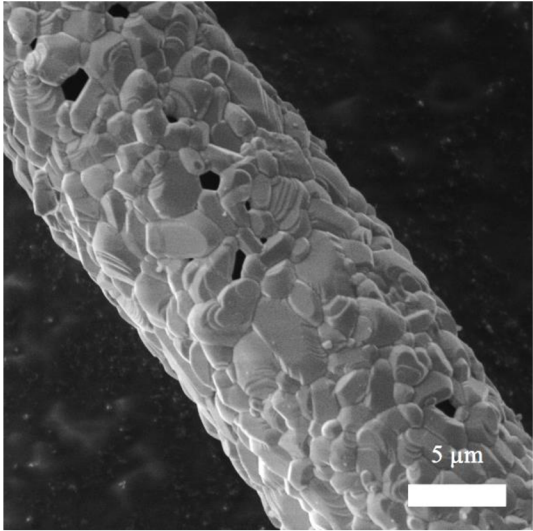
Outer diameter 13 μm,
rate of withdrawal 5 cm × s^{-1}.
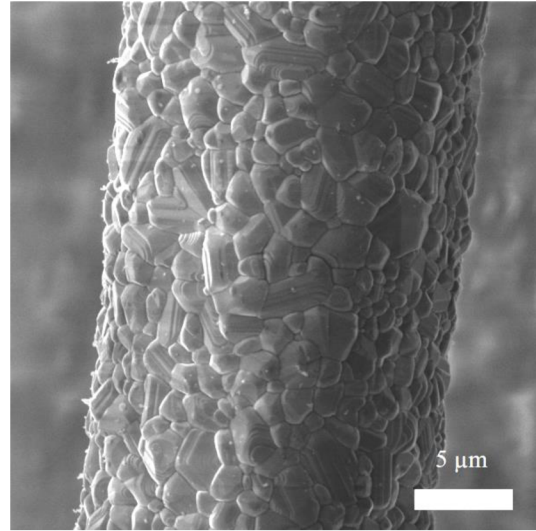
Outer diameter 16 μm,
rate of withdrawal 10 cm × s^{-1}.
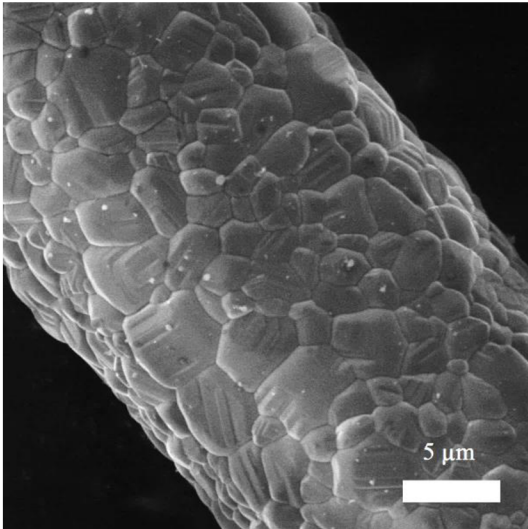
Outer diameter 21 μm,
rate of withdrawal 20 cm × s^{-1}.
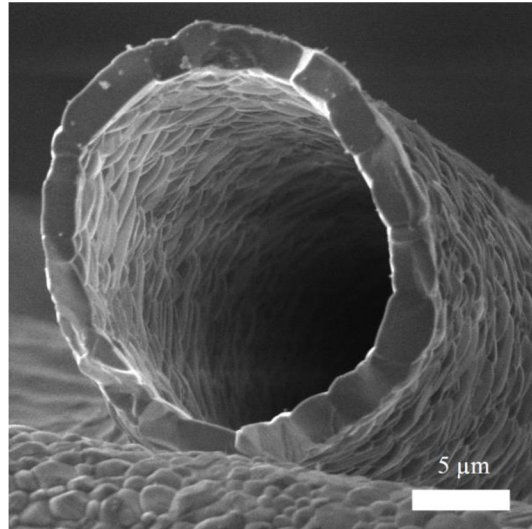
Cross section of dense hollow fiber,
rate of withdrawal 20 cm × s^{-1}.

Figure 41. The size of the grains of the ultrathin titania (10TiO2-1MC) hollow fiber
with a different diameter, sintered at 1200 ℃.

6 DISCUSION

6.1 Application of the sacrificial template

It is apparent from the results that it was possible to produce a thin wall ceramic hollow fibers using all three sacrificial templates. Each of the sacrificial templates carries its advantages and disadvantages in the production of these fibers.

UHMW PE fibers as a sacrificial template have problem with thermal expansion and relaxation of fiber at high temperatures. With increasing temperature and that increases in fiber diameter and the fiber relaxes. At low content of binder may occur crack that may be at a low coating thicknesses lead to collapse of structure. Another problem UHMW PE is the formation of drops at high rates of withdrawal, therefore it is necessary to focus on changing the viscosity of the material, one possibility is to increase the binder content. Higher content of methylcellulose results avoid droplet formation at high speeds while preventing cracking ceramic hollow fiber during sintering. Examples of collapsed structure, formed drops and stable film are shown in the Figure 29.

Cotton fibers as a sacrificial template have no problem with the formation of droplets due to the large diameter of fiber which only allowed the film to develop at the rates of withdrawal used. Also have no problem with cracking ceramic hollow fiber due less thermal expansion and relaxation fiber at high temperature due high content of binder used suspensions. Problem is loosely braided filaments of cotton, when suspension infiltrates into the spaces between filaments and after sintering there is no free channel but only the region of lower density material. This was prevented by pre-coating methylcellulose, which fills the free space and on the surface creates a thin protective film, which prevents suspension infiltration. Examples of ceramics fibers with region of lower density material and through channel are shown in the Figure 30 and Figure 31.

Carbon fibers as a sacrificial template allow the production of ceramic hollow fibers with a very thin wall, but their disadvantages are low mechanical properties due to the small diameter of the fiber and the impossibility of using a continuous coating. Another disadvantage is the high price compared to the two mentioned sacrificial templates. Thin wall ceramic hollow fibres produced by using carbon fiber are shown in the Figure 32.

The advantage of UHMW PE fiber is that it is relatively easy to handle and can be coated continuously. Another advantage is that it exists in variable diameters. In the case of use as a sacrificial template for fibers with a diameter 35 μm coatings can be achieved in the dimensions of tens of micrometers. However, it is necessary to use a suspension with a higher content of binders to prevent cracking of the resulting fibers. The high binder content results in a high viscosity of the suspension which prevents the formation of very thin films. Cotton fiber makes it possible to use

suspensions with a lower binder content, however due of the higher fiber diameter (170 µm) the resulting films are about 100 µm. The problem of the fibers also consists in the necessity of pre-coating with methylcellulose, which may not always be completely successful. When very low suspensions are used, the pre-coating need not be successful and fiber is infiltrated by suspensions. The carbon fiber has minimal thermal expansion and relaxation at high temperatures, thus allowing coatings very low viscosity suspension, also has small diameter (35 µm). This results in very thin films that are stable even after sintering and for these reasons appears to be the optimal sacrificial template. Problem is it is relatively hard to handle and does not allow continuous coating. The advantages and disadvantages of all sacrificed templates are summarized in the Table 15.

Table 15. Advantages and disadvantages of sacrificed templates.

Sacrificial template	Advantages	Disadvantages
UHMW PE fiber (35 µm)	very good mechanical properties, variable diameters	high thermal expansion and relaxation at high temperatures
Cotton fiber (170 µm)	good mechanical properties, low thermal expansion and relaxation at high temperatures	irregular shape, spaces between filaments and suspension infiltration
Carbon fiber (34.5 µm)	minimal thermal expansion and relaxation at high temperatures	poor mechanical properties, price

6.2 Dip-coating process

Using different suspensions and different rates of withdrawal we were able to achieve different coating thicknesses (5-53 µm, Table 11) and shapes (drop, film, Figure 29).

Our experiments demonstrated that increasing the drawing rate increases the thickness of the coating up to some level, see Figure 33. The increase is significant at first stage (up to 25 cm × s^{-1}, but at higher speeds the growth of the film is small or even thickness of coating decreases. These results coincide with the theory described above and summarized in the Figure 19 [34]. It is evident that after a sharp increase in film thickness (visco-inertial mode), at a certain rate the growth will stop or slightly decrease (boundary layer mode). First mode (visco-capillary) was not observed probably because of high viscosity of the suspensions. The viscosity varies with the withdraw rate of coating, as can be seen from the Figure 27, therefore suspensions are non-Newtonian fluids. This behavior is consistent with the above

mentioned literature [18]. It is evident that at lower withdrawal rates the behavior of non-Newtonian liquids is problematic, however at the applied withdrawal rates Newtonian behavior can be expected.

The suspensions used had an effect on the shape stability before and during sintering when increased binder content and therefore increased viscosity prevents the formation of drops during dip-coating and prevents collapse of the structure during sintering. When using low binder suspensions and therefore low viscosity, thin films (at low rates) and small drops (at high rates) are formed which collapses during sintering. This is shown in Figure 29. It is obvious that there is no universal ideal suspension, it is always necessary to take into account the properties of the sacrificial template and the desired thickness of the coating. Low viscosity suspensions work well and allow very thin films to be formed, but are prone to shape instability, and when an unsuitable template is used, the resulting structure collapses. High viscosity suspensions form only films, and if the binder content is sufficient, templates with high thermal expansion can be used. However, working with these suspensions is challenging, and can not be produced thin films such as low viscosity suspensions. It is always very important to adapt the composition of the suspension desired results.

6.3 Sintering of thin walls

Sintering for various grain size and porosity, expected behavior for relatively thick walls (over 100 μm). The grain size was within the range (0.3-0.9 μm) and the porosity in the range (2.6-18.4%).This is clearly shown in the Table 13 or in the Figure 34. These results are expected and coincide with the literature describing the sintering process [30].

Porosity is important for preparation of bio-scaffolds, therefore material were tested adhesion of cells to think wall ceramic hollow fibers from HAP. Fibers with outer diameter over 100 μm have mechanical strength sufficient to manipulation for biological testing. The cells adhere to hydroxyapatite without difficulty it is shown in Figure 36. This confirms the results of the work about building hydroxyapatite 3D scaffolds assembled from porous hollow fibers which uses hollow fibers to produce bioscaffold [36].

They were subsequently investigated TiO$_2$ hollow fibers with ultrathin wall (0.5-21 μm), densified at temperature 1200 °C. The grain size was then observed depending on the thickness of the wall, the thickness of the wall was controlled by the rate of withdrawal it is shown in Figure 39. The results show that grain size increases with increasing wall thickness as shown in the Table 14 or in the Figure 41.

This phenomenon is related to the problem of 3D and 2D thin film sintering. 3D sintering is faster because grain grows in all dimensions, 2D is slower because the grain can grow only in surface direction. The second impact on grain growth kinetics have inhomogeneous green body related to processing. In the process of producing

ceramic hollow fibers is one of the stages drying process of the coated layer. This process reduces volume of green body due to evaporation of water and thin film with higher density on the outer and inner surface is formed, see Figure 39. After subsequent sintering at 1200 °C this layer is dense and the grain coarsening occurs. In the case of thin ceramic hollow fibers, it is an endless thin film with the thickness of one grain only. At certain point sintering of ultrathin ceramic is changed from 3D to 2D sintering, which is slower due to longer diffusion path. Therefore, it can be concluded that the film is thinner, the faster 2D sintering occurs, and thus the grains coarsen slowly.

Comparison of 3D microstructures, surface and core titania block, are shown on the Figure 40. Surface is more dense due to evaporation and there are is only one side diffusion limitation, therefore surface grain size is significantly higher than in the core. Furthermore, inside 3D structure is porous and grains also limits each other's this leads to a slower sintering rate and smaller grains. That agree with the work that deals with the influence of porosity on sintering rates [30]. Comparison with bulk TiO$_2$ ceramics showed that the grain size of thin films does not reach the grain size on the surface of the bulk.

6.4   Location of the technology and potential of applications

Working with these ultrathin ceramic fibers is very challenging, because their dimensions are so small and poorly visible to the human eye. Thin walls also lead to very poor mechanical properties, making handling very demanding and limited. Another problem is also the low weight when handling very often they get into the lift if they lose contact with the pad.

In this work was presented a method of production of thin wall ceramic fibers. This method is unique because use thin fibers as sacrificial templates thanks to which these fibers can subsequently be hollow the size of the inner channel is determined by the size of the sacrificial template. Variations of rates of withdrawal and properties of the suspension, in particular the viscosity, can then be controlled by the resulting layer thickness. By adjusting a suitable sintering mode, subsequent porosity of the resulting ceramic fibers can be controlled.

Open cell ceramics are being used and considered for a variety of structural and nonstructural applications. Several methods can be used to produce ceramic materials in a cellular structure. The primary method of production of cellular ceramic materials is known as the "*replication*" process, or more specifically the "*polymer sponge*" process. These processes can result in foams with different ranges for characteristics such as relative density, proportion of open and closed cell faces, structure and morphology [8]. Our method results to ultrathin hollow ceramic fibers and uses fibers as the sacrificial templates. The difference is in the size of the pore when the foam has a minimum pore size of about 200 μm. Ultrathin hollow fibers

can reach a smaller pore size, however it is necessary gentle balance of forces in production.

Commercially available fibers are of the oxide (SiO_2, Al_2O_3) and non-oxide (S-C-O) nature and are produced by spinning. This method is common in ceramic fiber production but it is problematic to produce these fibers hollow. The CVD method another method for producing commercial ceramic fibers, similar as dip-coating uses the creating layers on the template (fiber), but the fiber then forms the core of the resulting ceramic fiber and its removal is problematic [32].

Another technique describes the work devoted solvent-based extrusion. This is a powder-based rapid prototyping process, the principle of which is the realization of liquid to solid transition through solvent evaporation in the presence of a binder. Extrusion can produce long fibers from powder suspensions, and allows them to build complex ceramic 3D structures and can be used in the fabrication of hard and soft tissue scaffolds. These extruded ceramic fibers can be hollow, but diameter of these fibers is much larger and lifetime of spinaret is limited. Al_2O_3-based suspensions were used in this work [37].

Another possibility was introduced at work about producing ceramic hollow fibers is non-solvent induced phase separation. The preparation method is based on dry-wet spinning of a particle-loaded polymer solution followed by thermal treatment. Resulting hollow fibers have small tunable radial dimensions, down to ~250 μm outer. The size of the inner canal is given by the separation and not sacrificial template and control of its size may be problematic. In this work were used ceramic materials Al_2O_3, SiC, YSZ and as metal nickel and stainless steel powder [38].

In summary we are not competing with the methods above, because our fiber dimensions are much smaller. Disadvantages of our process are limited sacrificial templates, diameter of these templates and their strength for continual coating. Also drying process is more sensitive. The thickness of the coating is limited by the fiber used and its diameter, shape quality (interaction suspension surface, not mentioned in theory). Another factor is the viscosity of the suspension used. These limits for UHMW PE fiber are shown in chapter 5.1.3.

The preparation of ceramic microchannel structures from powder based material was presented in work about microtemplating [39] where was produced ceramic alumina self-supporting microchannels structures with diameters from 10 to 1000 μm. Basis for this method is the controlled dip-coating of a sacrificial polymeric fiber template with suspensions containing sinterable particles. This work also mentions thermal expansion and gas production as an important factor in the sintering process. In this work Al_2O_3 was used in alcoholic suspensions. Presented results moved the limits set up in literature [39]. Our suspension are water-based which means better stability of the outer surface. Disadvantages are longer drying and difficult multicoating of the fiber and limited wall thickness.

Dip-coating is a simple and flexible process that can achieve hollow ceramic fibers with different wall sizes and through a subsequent sintering process of different porosity. Two materials (HAP, TiO_2) and three sacrifices fiber templates (UHMW PE, cotton, carbon fibers) were presented in this work. But other ceramic materials may be used, condition is to provide a suspension with suitable rheological properties and selecting a suitable sacrificial fiber template. There is a large number of these sacrificed fibers of different diameters, which can be used for dip-coating process. However, it is necessary to correctly evaluate the effect of their thermal expansion and relaxation at high temperatures.

Produced fibers hollow ceramic fibers can have many uses. Hydroxyapatite ceramic fibers can be used in production bio-scaffolds where a large surface, bioactive material is required. Titania fibers can be used in production photocatalytic cells which also require a large surface and a material capable of photocatalytic effect.

7 CONCLUSIONS

It can be concluded that the selection of suitable sacrificial template is the most important step for the production of ultrathin hollow ceramic fibers. The best choice as a sacrificial template appears to be carbon fiber which can be coated by very thin films and has no problems with thermal expansion and relaxation at high temperatures. However, the problem is the poor mechanical stability of the fiber due to its small diameter, which do not allows continuous coating, an alternative may be a UHMW fiber.

The dip-coating process was also successfully described. With the choice of a suitable suspension and rates of withdrawal, thin films can be formed. Due to the appropriate suspension composition, these ceramic hollow fibers have shape stability even after the subsequent sintering process.

Thin ceramic hollow fibers from hydroxyapatite with a porous structure have a potential application in production of bio-scaffolds. This is confirmed by successful biological test. Ultrathin ceramic hollow fibers prepared from titania have many applications, one of this is the study of sintering self-supporting structures with ultrathin walls.

The prepared fibers also have sufficient handling strength that can be controlled by adjusting the dip-coating process settings.

The presented method brings unique opportunity for preparation of ceramic self-supporting ceramic hollow fiber with dimension below 100 μm and wall thickness below 1 μm.

8 LITERATURE

[1] CALLISTER, William a David RETHWISCH. *Materials science and engineering: an introduction*. 8th ed. /. Hoboken, NJ: John Wiley, 2010. ISBN 04-704-1997-0.

[2] RAHAMAN, M. *Ceramic processing*. Boca Raton, FL: CRC/Taylor, 2007.

[3] PTÁČEK, Luděk. *Nauka o materiálu II*. 2. opr. a rozš. vyd. Brno: CERM, 2002. ISBN 80-720-4248-3.

[4] OZGÜR ENGIN, N. a A.Cüneyt TAS. Manufacture of macroporous calcium hydroxyapatite bioceramics. *Journal of the European Ceramic Society*. 1999, **19**(13-14), 2569-2572. DOI: 10.1016/S0955-2219(99)00131-4. ISSN 09552219. Dostupné také z: http://linkinghub.elsevier.com/retrieve/pii/S0955221999001314

[5] GOCKERT, Radek. *Tvarování biokeramiky metodou povlakování namáčením*. Brno, 2015. Bakalářská práce. Vysoké učení technické v Brně, Fakulta strojního inženýrství. Vedoucí práce Ing. David Salamon, Ph.D.

[6] HASHIMOTO, Kazuhito, Hiroshi IRIE a Akira FUJISHIMA. TiO 2 Photocatalysis: A Historical Overview and Future Prospects. *Japanese Journal of Applied Physics*. 2005, **44**(12), 8269-8285. DOI: 10.1143/JJAP.44.8269. ISSN 0021-4922. Dostupné také z: http://stacks.iop.org/1347-4065/44/8269

[7] ASKELAND, Donald, Pradeep FULAY a Wendelin WRIGHT. *The science and engineering of materials*. 6th ed. Stamford, CT: Cengage Learning, 2011. ISBN 04-952-9602-3.

[8] BROWN, David a David GREEN. Investigation of Strut Crack Formation in Open Cell Alumina Ceramics. *Journal of the American Ceramic Society*. 1994, **77**(6), 1467-1472. DOI: 10.1111/j.1151-2916.1994.tb09744.x. ISSN 0002-7820. Dostupné také z: http://doi.wiley.com/10.1111/j.1151-2916.1994.tb09744.x

[9] STUDART, Andre, Urs GONZENBACH, Elena TERVOORT a Ludwig GAUCKLER. Processing Routes to Macroporous Ceramics: A Review. *Journal of the American Ceramic Society*. 2006, **89**(6), 1771-1789. DOI: 10.1111/j.1551-2916.2006.01044.x. ISSN 0002-7820. Dostupné také z: http://doi.wiley.com/10.1111/j.1551-2916.2006.01044.x

[10] NOVOTNÁ, Lenka. *Biokeramické materiály pro pokročilé lékařské aplikace*. Brno, 2014. Pojednání ke státní doktorské zkoušce. Vysoké učení technické v Brně, Fakulta strojního inženýrství. Vedoucí práce Prof. RNDr. JAROSLAV CIHLÁŘ, CSc.

[11] OHJI, T a M FUKUSHIMA. Macro-porous ceramics: processing and properties. *International Materials Reviews*. 2013, **57**(2), 115-131. DOI: 10.1179/1743280411Y.0000000006. ISSN 0950-6608. Dostupné také z: http://www.tandfonline.com/doi/full/10.1179/1743280411Y.0000000006

[12] BONDERER, Lorenz, Philipp CHEN, Peter KOCHER a Ludwig GAUCKLER. Free-Standing Ultrathin Ceramic Foils. *Journal of the American Ceramic Society*. 2010, **93**(11), 3624-3631. DOI: 10.1111/j.1551-2916.2010.03927.x. ISSN 00027820. Dostupné také z: http://doi.wiley.com/10.1111/j.1551-2916.2010.03927.x

[13] LEWIS, Jennifer A. Colloidal Processing of Ceramics. *Journal of the American Ceramic Society*. 2000, **83**(10), 2341-2359. DOI: 10.1111/j.1151-2916.2000.tb01560.x. ISSN 00027820. Dostupné také z: http://doi.wiley.com/10.1111/j.1151-2916.2000.tb01560.x

[14] LIAO, D.L., G.S. WU a B.Q. LIAO. Zeta potential of shape-controlled TiO2 nanoparticles with surfactants. *Colloids and Surfaces A: Physicochemical and Engineering Aspects*. 2009, **348**(1-3), 270-275. DOI: 10.1016/j.colsurfa.2009.07.036. ISSN 09277757. Dostupné také z: http://linkinghub.elsevier.com/retrieve/pii/S0927775709004555

[15] SCHRIJNEMAKERS, A., S. ANDRÉ, G. LUMAY, N. VANDEWALLE, F. BOSCHINI, R. CLOOTS a B. VERTRUYEN. Mullite coatings on ceramic substrates: Stabilisation of Al2O3–SiO2 suspensions for spray drying of composite granules suitable for reactive plasma spraying. *Journal of the European Ceramic Society*. 2009, **29**(11), 2169-2175. DOI: 10.1016/j.jeurceramsoc.2009.01.031. ISSN 09552219. Dostupné také z: http://linkinghub.elsevier.com/retrieve/pii/S0955221909000491

[16] ZHANG, Jingxian, Masahiko MAEDA, Noriko KOTOBUKI, Motohiro HIROSE, Hajime OHGUSHI, Dongliang JIANG a Mikio IWASA. Aqueous processing of hydroxyapatite. *Materials Chemistry and Physics*. 2006, **99**(2-3), 398-404. DOI: 10.1016/j.matchemphys.2005.11.020. ISSN 02540584. Dostupné také z: http://linkinghub.elsevier.com/retrieve/pii/S0254058405007947

[17] HALLIDAY, David, Robert RESNICK a Jearl WALKER. *Fundamentals of physics*. 9th ed. Hoboken: John Wiley and Sons, 2011. ISBN 978-0-470-54791-5.

[18] JANALÍK, Jaroslav. *Viskozita tekutin a její měření* [online]. Ostrava: VŠB-TU Ostrava, Fakulta strojní, 2010, 66 s. [cit. 2017-02-22]. Dostupné z: http://docplayer.cz/14903740-Viskozita-tekutin-a-jeji-mereni.html

[19] FIALA, Jaroslav a Ivo KRAUS. *Povrchy a rozhraní*. Vyd. 1. Praha: České vysoké učení technické v Praze, 2009. ISBN 978-80-01-04248-9.

[20] KVÍTEK, Libor. *Metody studia koloidních soustav* [online]. Olomouc. PřF UP Olomouc: Katedra fyzikální chemie, 2006 [cit. 2017-02-26]. Dostupné z: http://chemikalie.upol.cz/skripta/msk/msk.pdf

[21] POINERN, Gérrard Eddy Jai, Ravi Krishna BRUNDAVANAM, Xuan THI LE, Philip K. NICHOLLS, Martin A. CAKE a Derek FAWCETT. The synthesis, characterisation and in vivo study of a bioceramic for potential tissue regeneration applications. *Scientific Reports*. 2014, **4**, 6235-. DOI: 10.1038/srep06235. ISSN 2045-2322. Dostupné také z: http://www.nature.com/articles/srep06235

[22] MOUSSA, Sana Ben, Hassen BACHOUâ, Michel GRUSELLE, Patricia BEAUNIER, Alexandrine FLAMBARD a Béchir BADRAOUI. Hybrid organic-inorganic materials based on hydroxyapatite structure. *Journal of Solid State Chemistry*. 2017, **248**, 171-177. DOI: 10.1016/j.jssc.2017.02.004. ISSN 00224596. Dostupné také z: http://linkinghub.elsevier.com/retrieve/pii/S0022459617300403

[23] RAPACZ-KMITA, A., C. PALUSZKIEWICZ, A. ŚLÓSARCZYK a Z. PASZKIEWICZ. FTIR and XRD investigations on the thermal stability of hydroxyapatite during hot pressing and pressureless sintering processes. *Journal of Molecular Structure*. 2005, **744-747**, 653-656. DOI: 10.1016/j.molstruc.2004.11.070. ISSN 00222860. Dostupné také z: http://linkinghub.elsevier.com/retrieve/pii/S0022286004009718

[24] TõNSUAADU, Kaia, Kārlis Agris GROSS, Liene PLūDUMA a Mihkel VEIDERMA. A review on the thermal stability of calcium apatites. *Journal of Thermal Analysis and Calorimetry*. 2012, **110**(2), 647-659. DOI: 10.1007/s10973-011-1877-y. ISSN 1388-6150. Dostupné také z: http://link.springer.com/10.1007/s10973-011-1877-y

[25] *ChemTube3D* [online]. Liverpool: University of Liverpool, b.r. [cit. 2017-03-05]. Dostupné z: http://www.chemtube3d.com

[26] CHEN, Xiaobo a Samuel S. MAO. Titanium Dioxide Nanomaterials: Synthesis, Properties, Modifications, and Applications. *Chemical Reviews*. 2007, **107**(7), 2891-2959. DOI: 10.1021/cr0500535. ISSN 0009-2665. Dostupné také z: http://pubs.acs.org/doi/abs/10.1021/cr0500535

[27] NAVRÁTIL, Vladislav a Lukáš PAWERA. *Fotokatalýza v praxi a ve škole* [online]. 1. vyd. Brno: Masarykova univerzita, 2014 [cit. 2017-03-05]. ISBN 978-80-210-7157-5.

[28] ZHANG, Hengzhong a Jillian F. BANFIELD. Thermodynamic analysis of phase stability of nanocrystalline titania. *Journal of Materials Chemistry*. 1998, **8**(9), 2073-2076. DOI: 10.1039/a802619j. ISSN 09599428. Dostupné také z: http://xlink.rsc.org/?DOI=a802619j

[29] KANG, Suk-Joong L. *Sintering: densification, grain growth, and microstructure*. 1st ed. Burlington: Elsevier Butterworth-Heinemann, 2005. ISBN 07-506-6385-5.

[30] MAYO, M. J. Processing of nanocrystalline ceramics from ultrafine particles. *International Materials Reviews*. 1996, **41**(3), 85-115. DOI: 10.1179/imr.1996.41.3.85. Dostupné také z: http://www.tandfonline.com/doi/full/10.1179/imr.1996.41.3.85

[31] PTÁČEK, Luděk. *Nauka o materiálu I.* 2., opr. a rozš. vyd. Brno: Akademické nakladatelství CERM, 2003. ISBN 80-720-4283-1.

[32] SCHAWALLER, Dirk, Bernd CLAUß a Michael R. BUCHMEISER. Ceramic Filament Fibers - A Review. *Macromolecular Materials and Engineering*. 2012, **297**(6), 502-522. DOI: 10.1002/mame.201100364. ISSN 14387492. Dostupné také z: http://doi.wiley.com/10.1002/mame.201100364

[33] KRENKEL, Walter. a Clauss BERND. *Ceramic matrix composites: Fiber reinforced ceramics and their applications*. Weinheim: Wiley-VCH, 2008. ISBN 978-3-527-31361-7.

[34] BOUWHUIS, Liesbeth. *Pebax composite mambranes for CO2 separations*. Twente, 2007, 100 s. Master thesis. University of Twente, Faculty of Science and Technology.

[35] *EN 623-3: Advanced technical ceramics-Monolithic ceramics-General and textural properties- Part 3: Determination of grain size and grain distribution (characterized by the linear intercept method).* 2001. Brusel: European Commitee for Standartiation, 2001.

[36] SALAMON, D., S. TEIXEIRA, S.M. DUTCZAK a D.F. STAMATIALIS. Facile method of building hydroxyapatite 3D scaffolds assembled from porous hollow fibers enabling nutrient delivery. *Ceramics International.* 2014, **40**(9), 14793-14799. DOI: 10.1016/j.ceramint.2014.06.071. ISSN 02728842. Dostupné také z: http://linkinghub.elsevier.com/retrieve/pii/S0272884214009663

[37] LU, Xuesong, Yoonjae LEE, Shoufeng YANG, Yang HAO, Julian R.G. EVANS a Clive G. PARINI. Solvent-based paste extrusion solid freeforming. *Journal of the European Ceramic Society.* 2010, **30**(1), 1-10. DOI: 10.1016/j.jeurceramsoc.2009.07.019. Dostupné také z: http://linkinghub.elsevier.com/retrieve/pii/S0955221909003860

[38] LUITEN-OLIEMAN, Mieke W.J., Michiel J.T. RAAIJMAKERS, Louis WINNUBST, Ton C. BOR, Matthias WESSLING, Arian NIJMEIJER a Nieck E. BENES. Towards a generic method for inorganic porous hollow fibers preparation with shrinkage-controlled small radial dimensions, applied to Al2O3, Ni, SiC, stainless steel, and YSZ. *Journal of Membrane Science.* 2012, **407-408**, 155–163. DOI: 10.1016/j.memsci.2012.03.030. Dostupné také z: http://linkinghub.elsevier.com/retrieve/pii/S0376738812002219

[39] SALAMON, David, Zdenek CHLUP, Leon LEFFERTS a Matthias WESSLING. Tailoring of free standing microchannels structures via microtemplating. *Materials Research Bulletin.* 2011, **46**(4), 505-511. DOI: 10.1016/j.materresbull.2011.01.005. Dostupné také z: http://linkinghub.elsevier.com/retrieve/pii/S0025540811000079

9 LIST OF FIGURES AND TABLES

10 LIST OF ABBREVIATIONS

Symbol	SI units	Description
dc/dx	[kg × m^{-4}]	gradient of concentration
du/dx	[s^{-1}]	gradient of speed
D	[m^2 × s^{-1}]	coefficient of diffusion
g	[m × s^{-2}]	gravitational acceleration
h	[m]	thickness of film
J	[kg × m^{-2} × s^{-1}]	diffuse flow
L	[m]	length of reservoirs
r	[m]	diameter of sacrificial fiber
T	[K]	temperature
v	[m × s^{-1}]	rate of withdrawal
γ	[N × m^{-2}]	surface tension
η	[Pa × s]	dynamic viscosity
ρ	[kg × m^{-3}]	density
τ	[Pa]	shear stress
ζ	[V]	zeta potential
Bo	[-]	Bond number
Ca	[-]	Capillary number
We	[-]	Weber number
κ^{-1}	[-]	capillary length

Abbreviation	Meaning
DLVO	Derjaguin, Landau, Verwey and Overbeek
ESA	Electrokinetic Sonic Amplitude
HAP	hydroxyapatite
IEP	isoelectric point
LLD	Landau, Levich and Deryagin
SEM	scanning electron microscopy
TiO$_2$	titania (titanium dioxide)
UHMW PE	ultra high molecular weight polyethylene